

## **An easy procedure to determine Magic Formula parameters: a comparative study between the starting value optimization technique and the IMMa optimization algorithm**

A. ORTIZ\*, J. A. CABRERA, A. J. GUERRA and A. SIMON

Department of Mechanical Engineering, University of Málaga, Campus El Ejido, 29013 Málaga, Spain

In 2004, a new searching algorithm for Magic Formula tyre model parameters was presented. Now, a summary of the results, for pure and combined slip, that this algorithm is able to achieve is presented. The Magic Formula tyre model needs a set of parameters to describe the tyre properties. The determination of these parameters is dealt with in this article. A new method, called IMMa Optimization Algorithm (IOA), based on genetic techniques, is used to determine these parameters. Here, we show the computational cost that has been used to obtain the optimum parameters of every characteristic of the Magic Formula tyre model, called Delft Tyre 96. The main advantages of the method are its simplicity of implementation and its fast convergence to optimal solution, with no need of deep knowledge of the searching space. Hence, to start the search, it is not necessary to know a set of starting values of the Magic Formula parameters (null sensitivity to starting values). The search can be started with a randomly generated set of parameters between [0, 1]. Nowadays, MF-Tool, an application developed by TNO, uses an optimization technique to fit Magic Formula parameters from Matlab toolbox [van Oosten, J.J.M. and Bakker, E., 1993, Determination of magic tyre model parameters. *Vehicle System Dynamics*, **21**, 19–29; van Oosten, J.J.M., Savi, C., Augustin, M., Bouhet, O., Sommer, J. and Colinot, J.P., 1999, Time, tire, measurements, forces and moments, a new standard for steady state cornering tyre testing. *EAEF Conference*, Barcelona, 30 June–2 July.]. We refer to that algorithm as the starting value optimization technique. The comparison between the optimization technique employed by TNO and the proposed IOA method is discussed in this article. In order to give a relative idea of adjustment accuracy, the sum-squared error and the mean-squared error, from the curves of the tyre model with the parameters optimized by both applications compared with test data are evaluated.

*Keywords:* Tyre; Tyre model; Optimization technique

### **1. Introduction**

Tyre models are used to calculate tyre forces and moments as responses to wheel motion that can be given in terms of various slip quantities. We can distinguish, in general, theoretical models, on the basis of physics of the tyre construction [1–4], and empirical or semi-empirical models solely on the basis of experimental results [5–6]. In addition, combinations of both approaches are used in the development of the tyre model.

---

\*Corresponding author. Email: aortizf@uma.es

A widely used empirical tyre model is based on the so-called Magic Formula [5]. The development of the model was done in a cooperative effort by the Delft University of Technology and Volvo Car Corporation. One of the latest versions is the so-called Delft Tyre 96 [9]. This model is capable of describing steady-state tyre force and moment characteristics in pure and combined slip conditions. Previously, Michelin introduced a purely empirical method using Magic Formula-based functions to describe tyre force generation in combined slip [6]. It implied a revolution in the conceptual way of considering combined slip. These tyre models use tyre measurement data as a basis. A set of Magic Formula parameters are derived from the tyre measurement data.

A procedure to find these parameters is by means of the starting value optimization (SVO) technique. In this approach a regression method is applied to the measurement data to derive the Magic Formula parameters. A main characteristic of this technique is that it requires starting values for the parameters to begin the optimization process. In the case of pure slip condition, most of the Magic Formula parameters have a physical meaning, so a good approximation of the starting values can be made. However, getting a set of good starting values for every tyre characteristic of the tyre model may be difficult, and normally the vehicle dynamics researching groups are not in possession of those. This is a limitation for the time needed to calculate the suitable parameters and to be successful in getting a global minimum.

The approach used in this article [8], to determine the Magic Formula parameters deals with genetic algorithms. Genetic algorithms were first introduced by Holland [9–10], whose work is included in Goldberg [11], and they have been extensively and successfully applied to different optimization problems. Our method defines a starting population that is improved by approximations to the goal function, making use of natural selection mechanisms and natural genetic laws. The main advantages of the IMM optimization algorithm (IOA) are its simplicity in implementing the algorithm and its low computational cost. Moreover, there is no need to have essential knowledge of either the searching space or the presence of local minima or other mathematical characteristics required for traditional searching algorithms, as well as of the goal function continuity. In addition, a good characteristic of the method presented is that it does not require starting values to begin the optimization process. This is an important feature because the user of this method does not necessarily have to know the physical characteristics of the Magic Formula parameters.

In this article, we make use of a set of test data that are courtesy from Hankook (Hankook 205/65R15 6.0J K406 RE tyre). For the longitudinal force, the test features are temperature (20 °C), velocity (65 km/h) and inflation pressure (2.2 bar). For the lateral force and aligning torque, the test features are temperature 20 °C, velocity 130 km/h and inflation pressure 2.2 bar.

This article is organized as follows: we establish a comparative study for longitudinal and lateral forces and for aligning torque between the results provided for the IOA and the SVO. To do so, we undertake comparative error estimation between the tyre test data and the tyre model curve generated with the parameters obtained by the SVO and the IOA for every tyre characteristic. According to this, we summarize the results. Later, we announce the general attributes for the IOA and finally we draw conclusions.

## 2. Procedure and cases

We use the IOA [8], to determine the Magic Formula parameters for pure and combined longitudinal and lateral forces and for auto-aligning torque [7], called Delft Tyre 96. The parameters obtained by our algorithm and by the SVO will be compared.

In addition, the starting population is initialized randomly between [0, 1] for all the cases. This is a feature of our algorithm. We do not need to know any physical properties and the

meaning of the tyre model parameters. Consequently, we need not select special and preferred values for the Delft Tyre 96 parameters for the searching initialization with the IOA.

**2.1 Case I: longitudinal force (pure longitudinal slip)**

Our algorithm uses the test data and the longitudinal force model to obtain a goal function. This goal function has the following scheme (equation (1)):

$$\min \sum_{i=1}^n \sum_{j=1}^m \left[ F_{x0}^{\text{Pacejka}}(X, \kappa_i, F_{z_j}) - F_{x0}^{\text{measured}}(\kappa_i, F_{z_j}) \right]^2 \tag{1}$$

where

$$X = \left\{ \begin{array}{l} \text{PCX1,} \\ \text{PDX1, PDX2,} \\ \text{PKX1, PKX2, PKX3,} \\ \text{PEX1, PEX2, PEX3, PEX4,} \\ \text{PHX1, PHX2,} \\ \text{PVX1, PVX2} \end{array} \right\}$$

$n$  is the number of longitudinal slip ratios in which the longitudinal force is evaluated for every vertical load,  $m$  is the number of load cases in which the longitudinal force is evaluated in the test procedure and  $X$  are the parameters for longitudinal force in the Delft Tyre 96.

The objective is reduced to search the  $X$  parameters that define the  $F_{x0}^{\text{Pacejka}}(X, \kappa_i, F_{z_j})$  function and that minimize the previous goal function in pure longitudinal slip conditions.

To do so, we only need to define the easy algorithm parameters: NP (population number) = 100,  $D$  (number of parameters to optimize) = 14,  $F$  (disturbing factor) = 0.6, CP (crossover probability) = 0.4, MP (mutation probability) = 0.1, range (mutation range) = 1 and itermax (number of iterations) = 1000.

With the objective to obtain the Magic Formula longitudinal force parameters, our algorithm was trained with the test data that correspond to three load cases, and the longitudinal slip ratio varied from  $-0.71$  to  $0.66$  in steps of  $0.01$  so that every longitudinal force curve was evaluated in 139 points.

**2.2 Case II: pure lateral force (pure side slip)**

Our algorithm uses the test data and the lateral characteristic of the tyre model to obtain a goal function. For the optimization of the lateral characteristic parameters, this goal function has the following scheme (equation (2)):

$$\min \sum_{i=1}^n \sum_{j=1}^m \sum_{g=1}^l \left[ F_{y0}^{\text{Pacejka}}(Y, \alpha_i, F_{z_j}, \gamma_g) - F_{y0}^{\text{measured}}(\alpha_i, F_{z_j}, \gamma_g) \right]^2 \tag{2}$$

where

$$Y = \left\{ \begin{array}{l} \text{PCY1,} \\ \text{PDY1, PDY2, PDY3} \\ \text{PKY1, PKY2, PKY3,} \\ \text{PEY1, PEY2, PEY3, PEY4,} \\ \text{PHY1, PHY2, PHY3} \\ \text{PVY1, PVY2, PVY3, PVY4} \end{array} \right\}$$

$n$  is the number of slip angles in which the lateral force is evaluated for every vertical load,  $m$  is the number of load cases,  $l$  are the numbers of camber angles in which the lateral force (pure side slip) is evaluated in the test procedure and  $Y$  are the parameters for lateral force in the Delft Tyre 96.

The objective is reduced to search the  $Y$  parameters that define the  $F_{y0}^{\text{Pacejka}}(Y, \alpha_i, F_{z_j}, \gamma_g)$  function and that minimize the previous goal function in pure side slip conditions.

To do so, we only need to define an easy algorithm parameter set: NP = 100,  $D = 18$ ,  $F = 0.6$ , CP = 0.4, MP = 0.1, range = 0.0003 and itermax = 2000.

With the objective to obtain the Magic Formula lateral force parameters, our algorithm was trained with the test data that correspond to five load cases and three camber angles, and the slip angle varied from  $-25^\circ$  to  $25^\circ$  so that every lateral force curve was evaluated in 82 points. Note that, here, the test data had an irregular distribution over the slip angle and the vertical load.

### 2.3 Case III: aligning torque (pure side slip)

Our algorithm uses the test data and the aligning torque characteristic of the tyre model to obtain a goal function. For the optimization of the aligning torque characteristic parameters, this goal function has the following scheme (equation (3)):

$$\min \sum_{i=1}^n \sum_{j=1}^m \sum_{g=1}^l \left[ M_{Z0}^{\text{Pacejka}}(Z, \alpha_i, F_{z_j}, \gamma_g) - M_{Z0}^{\text{measured}}(\alpha_i, F_{z_j}, \gamma_g) \right]^2 \quad (3)$$

where

$$Z = \left\{ \begin{array}{l} \text{PCY1,} \\ \text{PDY1, PDY2, PDY3} \\ \text{PKY1, PKY2, PKY3,} \\ \text{PEY1, PEY2, PEY3, PEY4,} \\ \text{PHY1, PHY2, PHY3} \\ \text{PVY1, PVY2, PVY3, PVY4} \\ \text{QBZ1, QBZ2, QBZ3, GBZ4, QBZ5} \\ \text{QCZ1} \\ \text{QDZ1, DDZ2, QDZ3, QDZ4} \\ \text{QEZ1, QEZ2, QEZ3, QEZ4, QEZ5} \\ \text{QHZ1, QHZ2, QHZ3, QHZ4} \\ \text{QBZ9, QBZ10} \\ \text{QDZ6, QDZ7, QDZ8, QDZ9} \end{array} \right\}$$

$n$  is the number of slip angles in which the autoaligning torque is evaluated for every vertical load,  $m$  is the number of load cases,  $l$  is the number of camber angles in which the aligning torque (pure side slip) is evaluated in the test procedure and  $Z$  are the parameters for the aligning torque in the Delft Tyre 96.

The objective is reduced to search the  $Z$  parameters that define the  $M_{Z0}^{\text{Pacejka}}(Z, \alpha_i, F_{z_j}, \gamma_g)$  function and that minimize the previous goal function in pure side slip conditions. In this case, we only need to look for the Q\*\*\* kind parameters with the IOA. The P\*\*\* kind parameters are same as those for lateral force.

To do so, we only need to define an easy algorithm parameter set: NP = 100,  $D = 25$ ,  $F = 0.6$ , CP = 0.4, MP = 0.1, range = 0.0003 and itermax = 3000.

With the objective to obtain the Magic Formula aligning torque parameters, our algorithm was trained with the test data that correspond to five load cases and seven camber angles, and

the slip angle varied from  $-25^\circ$  to  $25^\circ$  so that every aligning curve was evaluated in 82 points. We also trained the algorithm with the test data that correspond to three load cases and three camber angles, and the slip angle varied from  $-25^\circ$  to  $25^\circ$  so that every aligning curve was evaluated only in 16 points to show the dependency in time of the algorithm with the number of test data used to optimize the parameters. Note that, on this occasion, the test data also have an irregular distribution over the slip angle, the vertical load and the camber angle.

**2.4 Case IV: longitudinal force (combined slip)**

Our algorithm uses the test data and the longitudinal force model to obtain a goal function. This goal function has the following scheme (equation (4)):

$$\min \sum_{i=1}^n \sum_{j=1}^m \sum_{f=1}^p [F_x^{\text{Pacejka}}(X, \alpha_f, \kappa_i, F_{z_j}) - F_x^{\text{measured}}(\alpha_f, \kappa_i, F_{z_j})]^2 \tag{4}$$

where

$$X = \left\{ \begin{array}{l} \text{PCX1,} \\ \text{PDX1, PDX2,} \\ \text{PKX1, PKX2, PKX3,} \\ \text{PEX1, PEX2, PEX3, PEX4,} \\ \text{PHX1, PHX2,} \\ \text{PVX1, PVX2,} \\ \text{RCX1,} \\ \text{RHX1,} \\ \text{RBX1, RBX2} \end{array} \right\}$$

$n$  is the number of longitudinal slip ratios in which the longitudinal force is evaluated for every vertical load,  $m$  is the number of load cases,  $p$  is the number of slip angles in which the longitudinal force is evaluated in the test procedure and  $X$  are the parameters for longitudinal force in the Delft Tyre 96.

The objective is reduced to search the  $X$  parameters that define the  $F_x^{\text{Pacejka}}(X, \alpha_f, \kappa_i, F_{z_j})$  function and that minimize the previous goal function in combined slip conditions. In this case, we only need to look for the R\*\*\* kind parameters with the IOA. The P\*\*\* kind parameters are same as those for longitudinal force at pure slip conditions. Consequently, here IA0 has to optimize only four parameters.

To do so, we only need to define the easy algorithm parameters:  $NP = 100, D = 4, F = 0.6, CP = 0.4, MP = 0.15, \text{range} = 0.1$  and  $\text{itermax} = 1000$ .

With the objective to obtain the Magic Formula longitudinal force parameters in the combined slip, our algorithm was trained with the test data that correspond to three load cases and seven different slip angles, and the longitudinal slip ratio varied from  $-0.71$  to  $0.66$  in steps of  $0.01$  so that every longitudinal force curve was evaluated in 139 points.

**2.5 Case V: lateral force (combined slip)**

Our algorithm uses the test data and the lateral characteristic of the tyre model to obtain a goal function. For the optimization of the lateral characteristic parameters, this goal function has the following scheme (equation (5)):

$$\min \sum_{i=1}^n \sum_{j=1}^m \sum_{f=1}^p [F_y^{\text{Pacejka}}(Y, \kappa_i, \alpha_f, F_{z_j}) - F_y^{\text{measured}}(\kappa_i, \alpha_f, F_{z_j})]^2 \tag{5}$$

where

$$Y = \left\{ \begin{array}{l} \text{PCY1,} \\ \text{PDY1, PDY2, PDY3} \\ \text{PKY1, PKY2, PKY3,} \\ \text{PEY1, PEY2, PEY3, PEY4,} \\ \text{PHY1, PHY2, PHY3} \\ \text{PVY1, PVY2, PVY3, PVY4} \\ \text{RBY1, RBY2, RBY3} \\ \text{RCY1} \\ \text{RHY1} \\ \text{RVY1, RVY2, RVY3, RVY4, RVY5, RVY6} \end{array} \right\}$$

$n$  is the number of longitudinal slip ratios in which the lateral force is evaluated for every vertical load,  $m$  is the number of vertical load cases,  $p$  is the number of slip angles in which the lateral force for combined slip condition is evaluated in the test procedure and  $Y$  are the parameters for lateral force in the Delft Tyre 96.

The objective is reduced to search the  $Y$  parameters that define the  $F_y^{\text{Pacejka}}(Y, \kappa_i, \alpha_f, F_{z_j})$  function and that minimize the previous goal function in combined slip condition. In this case, we only need to look for the R\*\*\* kind parameters with the IOA. The P\*\*\* kind parameters are same as those for lateral force in pure side slip conditions. Consequently, here, IAO has to optimize only 11 parameters.

To do so, we only need to define an easy algorithm parameter set: NP = 100,  $D = 11$ ,  $F = 0.6$ , CP = 0.4, MP = 0.1, range = 0.003 and itermax = 1000.

With the objective to obtain the Magic Formula lateral force parameters, our algorithm was trained with the test data that correspond to three load cases and six slip angles, and the longitudinal slip ratio varied from  $-0.71$  to  $0.66$  in steps of  $0.01$  so that every lateral force curve was evaluated in 139 points.

### 3. Results

These parameters have been optimized with the following tyre test data units: length (m), force (N), angle (rad), mass (kg), time (s) and  $\kappa(-)$ .

The algorithm was programmed in an Intel Pentium 4 (CPU 2.00 GHz and 768 MB RAM) and implemented in Matlab.

The computational time is highly dependent on the number of test points in which the goal function is minimized, and the number of parameters to be optimized is an influential element in the computational cost. Obviously, NP of the starting population is also relevant to this subject.

#### 3.1 Case I

The results obtained in this case are presented in figure 1. Here, it is possible to observe the different adjustment that the Magic Formula for pure longitudinal slip has to the tyre test data if the IOA and the SVO are used to optimize the Magic Formula parameters.

Note that in figure 1, there are not 139 test points represented for every vertical load, with the objective to clarify the figure.

For the Magic Formula Delft Tyre 96 version, the longitudinal force parameters optimized by our algorithm and the ones obtained by SVO are presented in table 1.

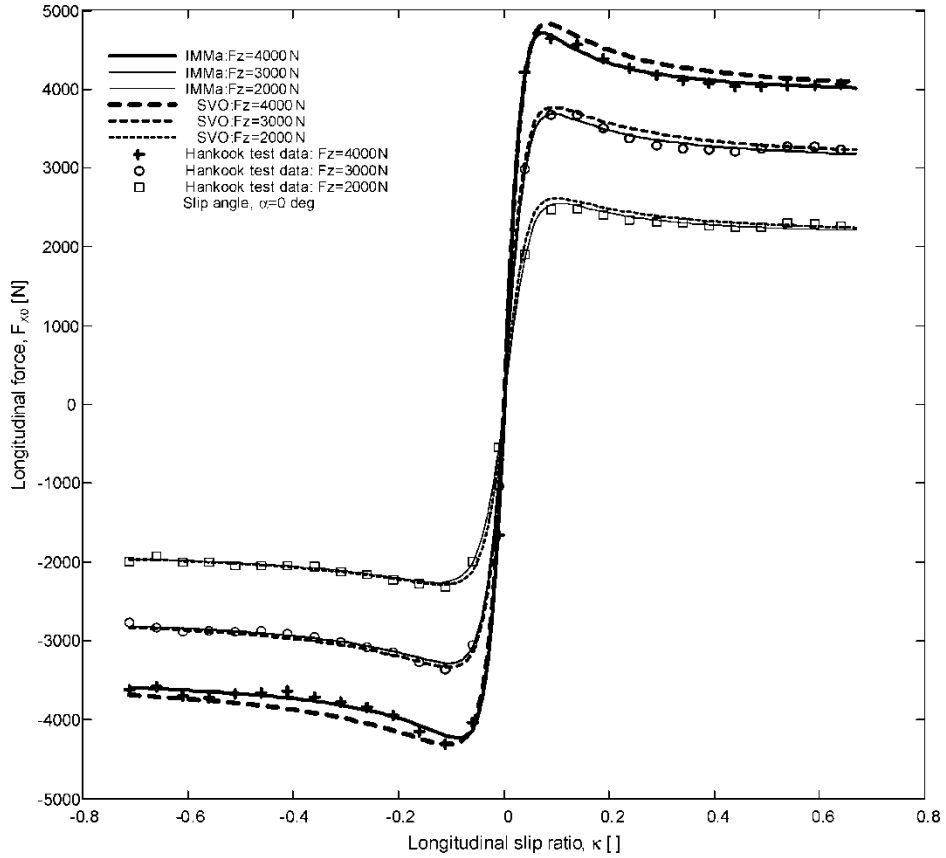


Figure 1. Longitudinal force comparison obtained with parameters optimized by the IMMa algorithm and the SVO.

Table 1. Longitudinal force parameters (pure longitudinal slip) of the Magic Formula Delft Tyre 96 version.

Longitudinal coefficients	SVO	IMMa algorithm
PCX1: $C_{F_x}$ shape factor for longitudinal force	1.4146	1.39708965522517
PDX1: $\mu_x$ longitudinal friction at $F_{znom}$	1.1264	1.10206790799301
PDX2: $\mu_x$ friction variation with load	-0.18176	-0.18524061849074
PEX1: $E_{F_x}$ longitudinal curvature at $F_{znom}$	0.001242	-0.45925516498559
PEX2: $E_{F_x}$ curvature variation with load	0.004268	-1.49950140524233
PEX3: $E_{F_x}$ curvature variation with squared load	0.005999	-2.46964541360566
PEX4: Factor in $E_{F_x}$ curvature while driving	314.36	-0.90674124856268
PKX1: $K_{F_x}/F_z$ longitudinal slip stiffness at $F_{znom}$	36.12	38.50310903831592
PKX2: $K_{F_x}/F_z$ slip stiffness variation with load	11.489	2.03196267718832
PKX3: Exponent in $K_{F_x}/F_z$ slip stiffness with load	0.1678	-0.59108577080244
PHX1: $S_{hx}$ horizontal shift at $F_{znom}$	-0.0017105	-0.00227143201428
PHX2: $S_{hx}$ shift variation with load	0.0030235	0.00193554524925
PVX1: $S_{vx}/F_z$ vertical shift at $F_{znom}$	0.06054	0.05759227819402
PVX2: $S_{vx}/F_z$ shift variation with load	-0.03904	-0.02874956840315

Table 2. Sum-squared error from the longitudinal force curve to the longitudinal force test data.

	Sum-squared error (N <sup>2</sup> )	
	$\sum_{i=1}^n \sum_{j=1}^m [F_{x0}^{IMMa \text{ algorithm}} - F_{x0}^{\text{measured}}]^2$	$\sum_{i=1}^n \sum_{j=1}^m [F_{x0}^{SVO} - F_{x0}^{\text{measured}}]^2$
$F_z = [4000, 3000, 2000]N$ $-0.71 \leq \kappa \leq 0.66$	$1.169481 \times 10^6$	$4.266528 \times 10^6$

Table 3. MSE from the longitudinal force curve to the longitudinal force tyre test data expressed in rate percentage.

	% MSE	
	$\sqrt{\left[ \frac{\sum_{i=1}^n (F_{x0}^{IMMa \text{ algorithm}} - F_{x0}^{\text{measured}})^2}{\sum_{i=1}^n (F_{x0}^{\text{measured}})^2} \right]}$	$\sqrt{\left[ \frac{\sum_{i=1}^n (F_{x0}^{SVO} - F_{x0}^{\text{measured}})^2}{\sum_{i=1}^n (F_{x0}^{\text{measured}})^2} \right]}$
$F_z = 4000 \text{ N}$	1.53	3.47
$F_z = 3000 \text{ N}$	1.74	2.68
$F_z = 2000 \text{ N}$	1.98	3.25
Total	1.75	3.13

The IOA took a computational time of 5 min 47 s when  $n$  was 139 points and  $m$  was three load cases.

With the aim to evaluate the quality of the adjustment to the tyre test data, we have evaluated the sum-squared differences between the longitudinal forces with the parameters optimized

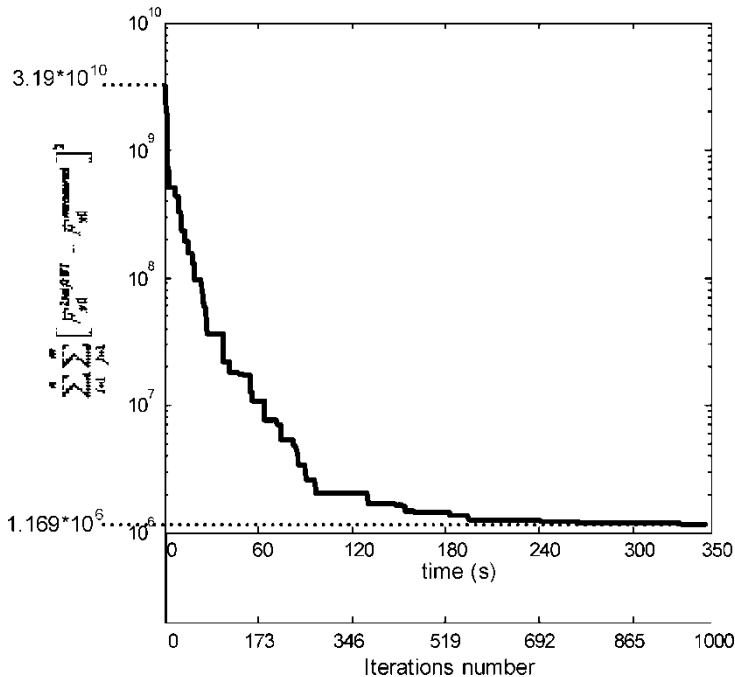


Figure 2. Development of the sum-squared error for longitudinal force along 1000 iterations and accumulated for 139 points and three vertical load cases.



by the SVO and the IMMa algorithm. The results can be observed in table 2. The sum of all the differences from the test data to the longitudinal force curve obtained with the IMMa algorithm is approximately one-third of the error compared with the result obtained with Magic Formula tyre application.

In addition, the mean-squared error (MSE), between the test data and the longitudinal force curve, which correspond to the parameters obtained with every searching procedure, has been evaluated and expressed in rate percentage for every load case and for the total in table 3. We observe a better adjustment to the tyre test data, using the searching algorithm proposed in this article, from evidences from tables 2 and 3.

During the time the algorithm worked, the sum-squared error evolved as shown in figure 2. The time the IOA spent searching the optimum parameters is overestimated. The final sum-squared error does not go down once 519 iterations have been exceeded. The algorithm took only 180 s to realize approximately 500 iterations.

### 3.2 Case II

The results obtained for camber angle  $\gamma = 0$  are presented in figure 3. The results obtained for camber angles  $2^\circ$  and  $4^\circ$  are presented in figures 4 and 5, respectively. For every camber angle, it is possible to observe the different adjustment that the Magic Formula lateral force

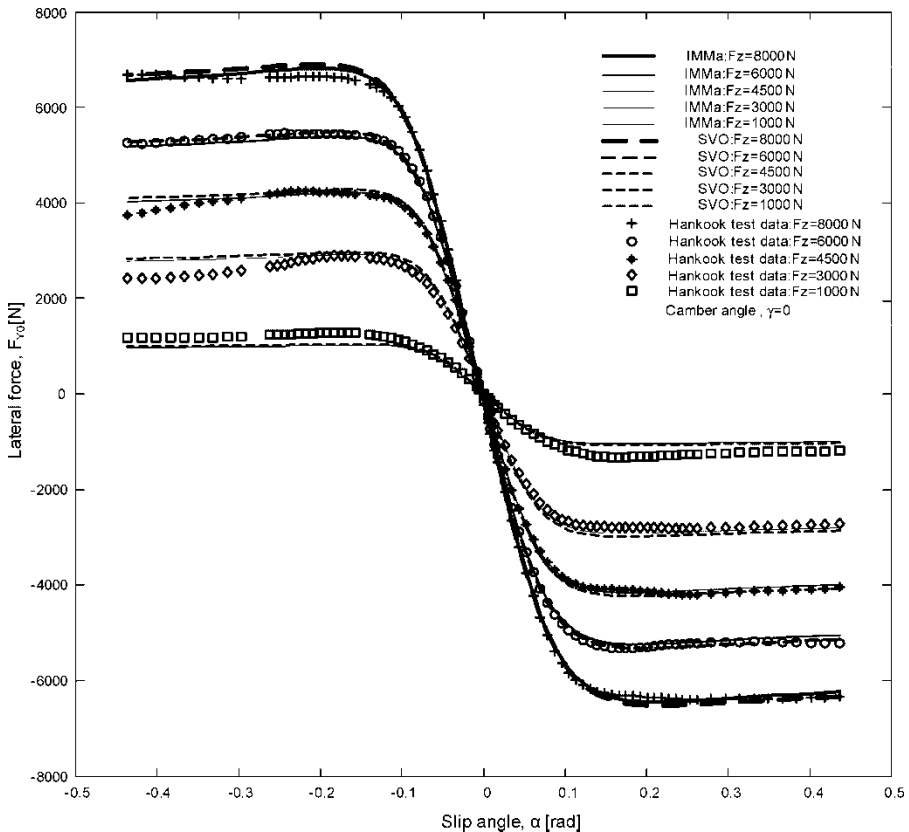


Figure 3. Lateral force comparison obtained with the parameters optimized by the IMMa algorithm and the SVO with respect to  $\gamma = 0^\circ$  test data.

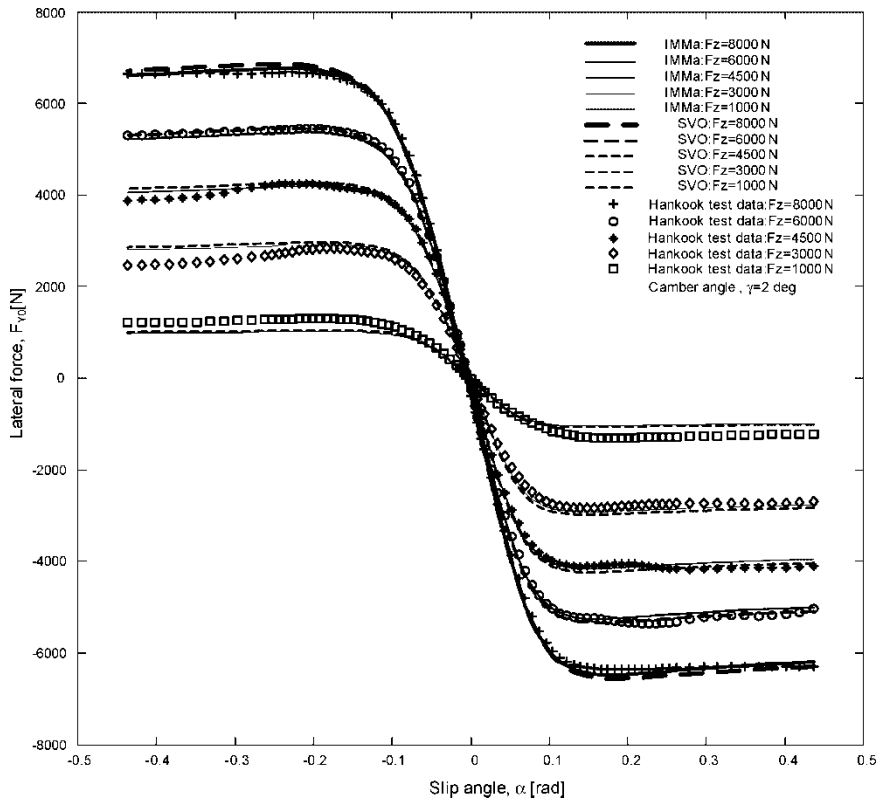


Figure 4. Lateral force comparison obtained with parameters optimized by the IMMa algorithm and the SVO with respect to  $\gamma = 2^\circ$  test data.

for pure side slip has to the tyre test data if the IOA and the SVO are used to optimize the Magic Formula parameters.

For the Magic Formula Delft Tyre 96 version, the lateral force parameters optimized by our algorithm and the ones obtained by the SVO are presented in table 4.

The algorithm took a computational time of 5 min 47 s when  $n$  was 82 points,  $m$  was five load cases and  $l$  was three camber angles.

With the aim to evaluate the quality of adjustment to the tyre test data, we have evaluated the sum-squared differences between the lateral forces with the parameters optimized by the SVO and the IMMa algorithm. The results can be observed in table 5. The sum of all the differences from the test data to the lateral force curve obtained with the IMMa algorithm is 78% of the error obtained with the SVO.

Also, the MSE between the lateral force test data and the lateral force curve obtained with the parameters that correspond to every searching procedure has been evaluated and expressed in rate percentage for the total in table 6, and every vertical load case and camber angles  $0^\circ$ ,  $2^\circ$  and  $4^\circ$  are shown in tables 7–9, respectively.

For the  $\gamma$  camber angles  $-4^\circ$ ,  $-2^\circ$ ,  $-1^\circ$ ,  $0^\circ$ ,  $4^\circ$ ,  $2^\circ$  and  $1^\circ$ , we observe a better adjustment to the lateral force test data, using the searching algorithm based on genetics proposed in this article, even though the algorithm has been trained only with the tyre test data that correspond to the  $\gamma$  camber angles  $-4^\circ$ ,  $0^\circ$  and  $4^\circ$ .

In table 8, it is observed that the MSE with the IOA is lower than the MSE with SVO, even though the IOA was not trained with the test data that correspond with  $\gamma = 2^\circ$ . Owing to this,

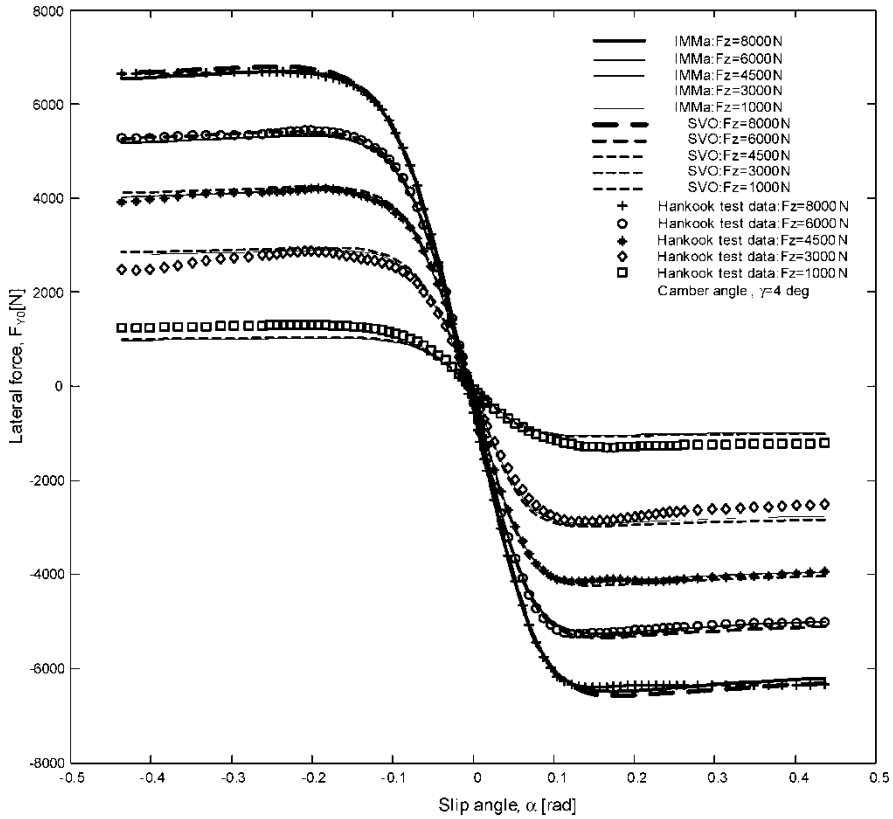


Figure 5. Lateral force comparison obtained with parameters optimized by the IMMa algorithm and the SVO with respect to  $\gamma = 4^\circ$  test data.

Table 4. Lateral force parameters (pure side slip) of the Magic Formula Delft Tyre 96 version.

Longitudinal coefficients	SVO	IMMa algorithm
PCY1: $C_{FY}$ shape factor for lateral force	1.2664	1.27676
PDY1: $\mu_Y$ lateral friction	0.949	0.9327755
PDY2: $\mu_Y$ friction variation with load	-0.13463	-0.128085
PDY3: $\mu_Y$ friction variation with square camber	0.8261	1.019803
PEY1: Lateral $E_{FY}$ curvature at $F_{znom}$	-1.3159	-1.39934
PEY2: $E_{FY}$ curvature variation with load	-0.4004	-0.074863
PEY3: Zero order camber dependency of $E_{FY}$ curvature	0.1824	0.17886
PEY4: $E_{FY}$ curvature variation with camber	-8.101	-8.252847
PKY1: $K_{FY}/F_{znom}$ stiffness maximum value	-16.832	-17.361823
PKY2: Load at which $K_{FY}/F_{znom}$ reaches maximum value	2.101	2.2938964
PKY3: $K_{FY}/F_{znom}$ variation with camber	-0.10954	-0.110362
PHY1: $S_{hY}$ horizontal shift at $F_{znom}$	0.0015064	0.0016966
PHY2: $S_{hY}$ shift variation with load	0.0043944	0.0038829
PHY3: $S_{hY}$ shift variation with camber	0.03976	0.0398737
PVY1: $S_{vY}/F_z$ vertical shift at $F_{znom}$	0.005431	0.0069311
PVY2: $S_{vY}/F_z$ shift variation with load	0.022704	0.0186856
PVY3: $S_{vY}/F_z$ shift variation with camber	-0.0771	-0.061575
PVY4: $S_{vY}/F_z$ shift variation with camber and load	-0.09083	-0.098064

Table 5. Sum-squared error from lateral force curve to lateral force test data.

	Sum-squared error (N <sup>2</sup> )	
	$\sum_{i=1}^n \sum_{j=1}^m \sum_{g=1}^l \left[ F_{y0}^{\text{IMMa algorithm}} - F_{y0}^{\text{measured}} \right]^2$	$\sum_{i=1}^n \sum_{j=1}^m \sum_{g=1}^l \left[ F_{y0}^{\text{SVO}} - F_{y0}^{\text{measured}} \right]^2$
$F_z = [8000, 6000, 4500, 3000, 1000] \text{ N}$ $-25^\circ \leq \alpha \leq 25^\circ$ $\gamma = [-4, 0, 4]^\circ$	$1.8725490 \times 10^7$	$2.3860189 \times 10^7$

Table 6. MSE from the lateral force curve to the lateral force test data expressed in rate percentage for all vertical loads and all camber angles.

	% MSE	
	$\sqrt{\left[ \frac{\sum_{i=1}^n (F_{y0}^{\text{IMMa algorithm}} - F_{y0}^{\text{measured}})^2}{\sum_{i=1}^n (F_{y0}^{\text{measured}})^2} \right]}$	$\sqrt{\left[ \frac{\sum_{i=1}^n (F_{y0}^{\text{SVO}} - F_{y0}^{\text{measured}})^2}{\sum_{i=1}^n (F_{y0}^{\text{measured}})^2} \right]}$
$F_z = [8000, 6000, 4500, 3000, 1000] \text{ N}$ $-25^\circ \leq \alpha \leq 25^\circ$ $\gamma = [-4, -2, -1, 0, 4, 2, 1]^\circ$	5.88	6.08

Table 7. MSE from the lateral force curve to the lateral force test data expressed in rate percentage for  $\gamma = 0^\circ$ .

	% MSE	
$\gamma = 0^\circ$	$\sqrt{\left[ \frac{\sum_{i=1}^n (F_{y0}^{\text{IMMa algorithm}} - F_{y0}^{\text{measured}})^2}{\sum_{i=1}^n (F_{y0}^{\text{measured}})^2} \right]}$	$\sqrt{\left[ \frac{\sum_{i=1}^n (F_{y0}^{\text{SVO}} - F_{y0}^{\text{measured}})^2}{\sum_{i=1}^n (F_{y0}^{\text{measured}})^2} \right]}$
$F_z = 8000 \text{ N}$	1.48	2.35
$F_z = 6000 \text{ N}$	1.53	0.67
$F_z = 4500 \text{ N}$	1.96	2.60
$F_z = 3000 \text{ N}$	5.52	7.41
$F_z = 1000 \text{ N}$	17.82	15.95
Total	5.66	5.80

Table 8. MSE from the lateral force curve to the lateral force test data expressed in rate percentage for  $\gamma = 2^\circ$ .

	% MSE	
$\gamma = 2^\circ$	$\sqrt{\left[ \frac{\sum_{i=1}^n (F_{y0}^{\text{IMMa algorithm}} - F_{y0}^{\text{measured}})^2}{\sum_{i=1}^n (F_{y0}^{\text{measured}})^2} \right]}$	$\sqrt{\left[ \frac{\sum_{i=1}^n (F_{y0}^{\text{SVO}} - F_{y0}^{\text{measured}})^2}{\sum_{i=1}^n (F_{y0}^{\text{measured}})^2} \right]}$
$F_z = 8000 \text{ N}$	1.55	2.35
$F_z = 6000 \text{ N}$	1.95	1.25
$F_z = 4500 \text{ N}$	2.43	2.90
$F_z = 3000 \text{ N}$	5.66	7.58
$F_z = 1000 \text{ N}$	19.07	17.18
Total	6.13	6.25

Table 9. MSE from the lateral force curve to the lateral force test data expressed in rate percentage for  $\gamma = 4^\circ$ .

$\gamma = 4^\circ$	% MSE	
	$\sqrt{\left[ \frac{\sum_{i=1}^n (F_{y0}^{IMMa \text{ algorithm}} - F_{y0}^{\text{measured}})^2}{\sum_{i=1}^n (F_{y0}^{\text{measured}})^2} \right]}$	$\sqrt{\left[ \frac{\sum_{i=1}^n (F_{y0}^{SVO} - F_{y0}^{\text{measured}})^2}{\sum_{i=1}^n (F_{y0}^{\text{measured}})^2} \right]}$
$F_z = 8000 \text{ N}$	1.15	1.71
$F_z = 6000 \text{ N}$	1.28	1.44
$F_z = 4500 \text{ N}$	1.14	2.15
$F_z = 3000 \text{ N}$	5.73	7.88
$F_z = 1000 \text{ N}$	19.34	17.40
Total	5.73	6.12

the IOA is capable of finding an optimal solution with parameters useful for vertical load cases that were not employed in the optimization process.

During the time the algorithm worked, the sum-squared error for lateral force evolved as shown in figure 6.

The time the IOA spent searching the optimum  $Y$  parameters is overestimated. The final sum-squared error does not go down once 350 iterations have been exceeded. The algorithm took only 60 s to realize approximately 350 iterations to obtain the final solution.

### 3.3 Case III

The results obtained for  $\gamma = 0^\circ$  camber angle are presented in figure 7. The results obtained for camber angles  $2^\circ$  and  $4^\circ$  are presented in figures 8 and 9, respectively. For every camber

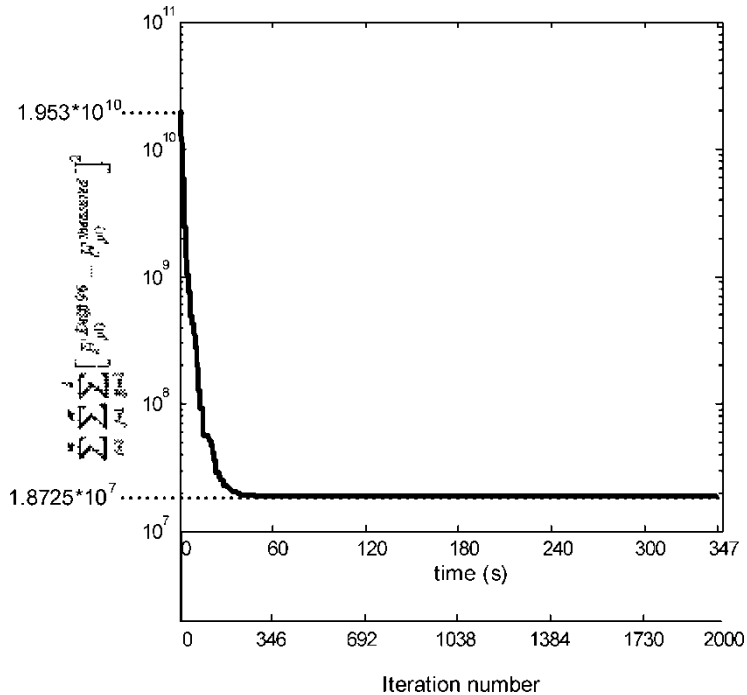


Figure 6. Sum-squared error development for lateral force along 2000 iterations accumulated for 82 test points for every vertical load and five vertical load cases and three different camber angles.

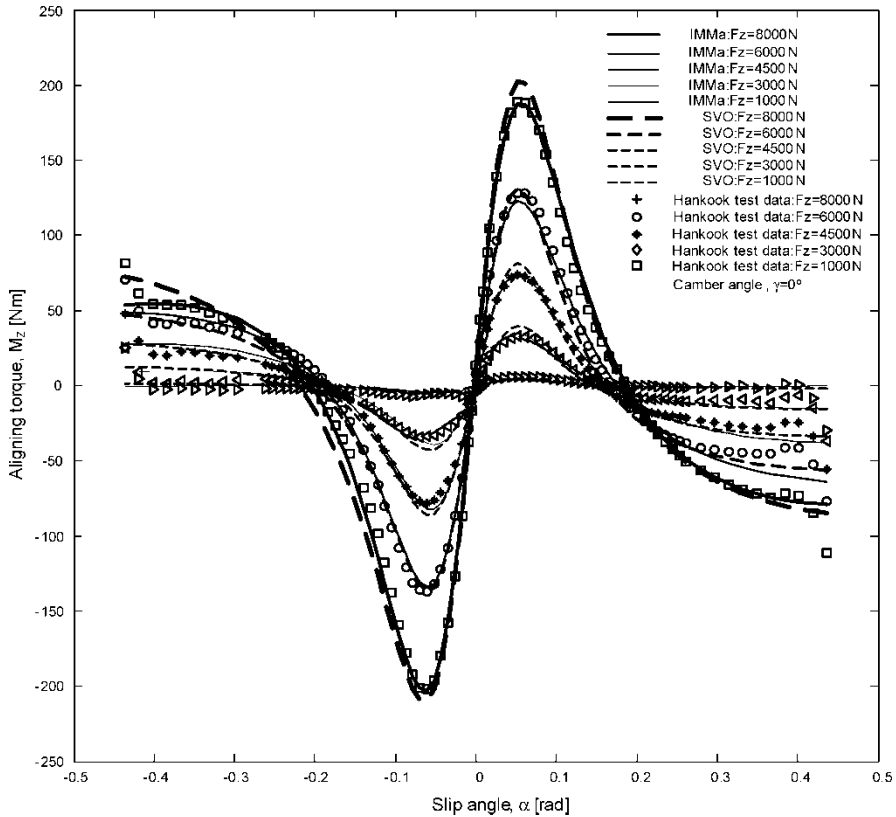


Figure 7. Aligning torque comparison obtained with parameters optimized by the IMMa algorithm and the SVO with respect to  $\gamma = 0^\circ$  test data.

angle, it is possible to observe a different adjustment that the Magic Formula aligning torque for pure side slip has to the tyre test data if IMMa algorithm and the SVO are used to optimize the Magic Formula parameters. These results correspond to the first training process of both discussed previously. The second one gives very similar results to those of figures 7–9.

For the Magic Formula Delft Tyre 96 version, the aligning torque parameters optimized by our algorithm and the ones obtained by the SVO are presented in table 10.

The algorithm took a computational time of 47 min 52 s when the number of iterations was 3000,  $n$  was 82 points,  $m$  was five load cases and  $l$  was seven camber angles. The computational time is highly dependent on the number of points where the goal function is minimized. Owing to this, the computational time went down to 7 min 53 s when the number of iterations was 3000,  $n$  was 16 points,  $m$  was three load cases and  $l$  was three camber angles.

The aligning torque coefficients presented in table 10 belong to the Z parameters obtained when the IMMa algorithm ran under the conditions of the first case mentioned earlier.

With the goal to evaluate the quality of adjustment to the tyre test data, we have evaluated the sum-squared differences between the aligning torque curve obtained with the parameters optimized by the SVO and the IMMa algorithm. The results can be observed in table 11. In this case, these sum-squared differences are presented in two different situations, evaluating 82 and 16 points for every vertical load.

The sum of all the differences from the test data to the aligning torque curve obtained with the parameters optimized by IMMa algorithm is 65% of the error compared with the result

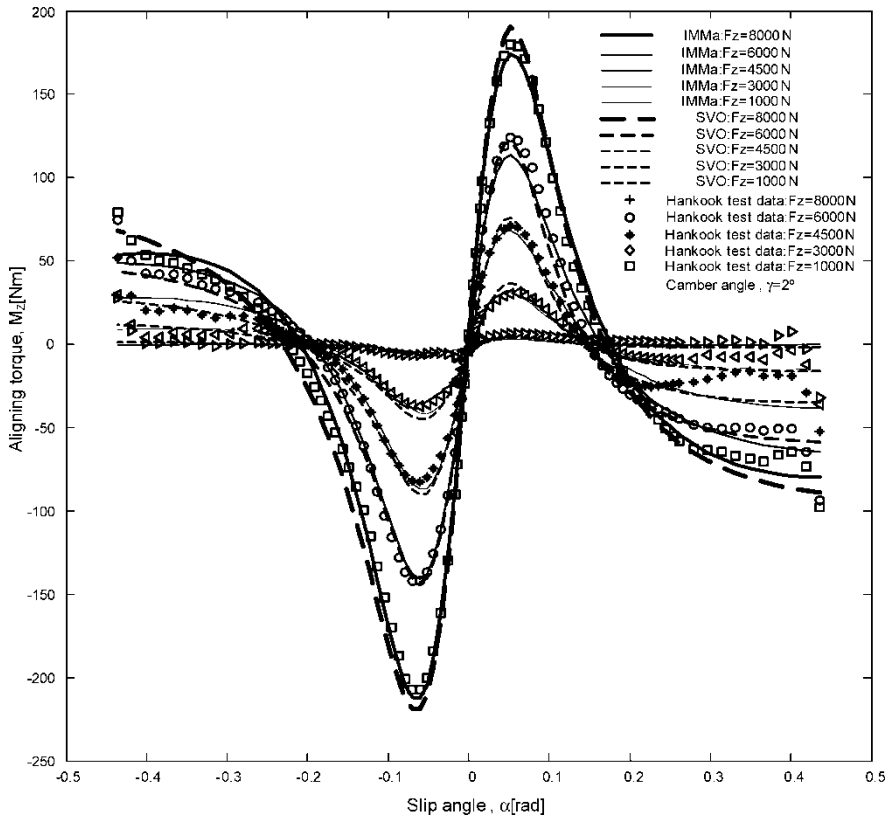


Figure 8. Aligning torque comparison obtained with parameters optimized by the IMMa algorithm and the SVO with respect to  $\gamma = 2^\circ$  test data.

obtained with the parameters optimized by the SVO in the case of 82 points for every vertical load and 30% for 16 points for every vertical load.

The IMMa algorithm is able to obtain a set of optimum Z parameters, using only 16 values of aligning torque for every vertical load and every camber angle, besides using only three vertical loads and three cases of camber angles. This option allows getting the solution with less computational time at the expense of a greater MSE.

In addition, the MSE between the aligning torque test data and the aligning torque curve obtained with the parameters that correspond to every searching procedure has been evaluated and expressed in rate percentage for the total in table 12, and every vertical load case and camber angles  $0^\circ$ ,  $2^\circ$  and  $4^\circ$  are shown in tables 13–15 respectively.

For the  $\gamma$  camber angles  $-4^\circ$ ,  $-2^\circ$ ,  $-1^\circ$ ,  $0^\circ$ ,  $4^\circ$ ,  $2^\circ$  and  $1^\circ$ , we observe a better adjustment to the aligning torque test data, using the searching algorithm based on genetics proposed in this article. The algorithm has been trained with the tyre test data that correspond to the  $\gamma$  camber angles  $-4^\circ$ ,  $-2^\circ$ ,  $-1^\circ$ ,  $0^\circ$ ,  $1^\circ$ ,  $2^\circ$  and  $4^\circ$  and with vertical loads 8000, 6000, 4500, 3000 and 1000 N.

During the time the algorithm worked, the sum-squared error for the aligning torque evolved as shown in figure 10. The time the IOA spent searching the optimum parameters is overestimated.

The final sum-squared error did not go down once 1253 iterations were exceeded. The algorithm took 20 min to realize 1253 iterations to obtain the final solution. Note that, in this

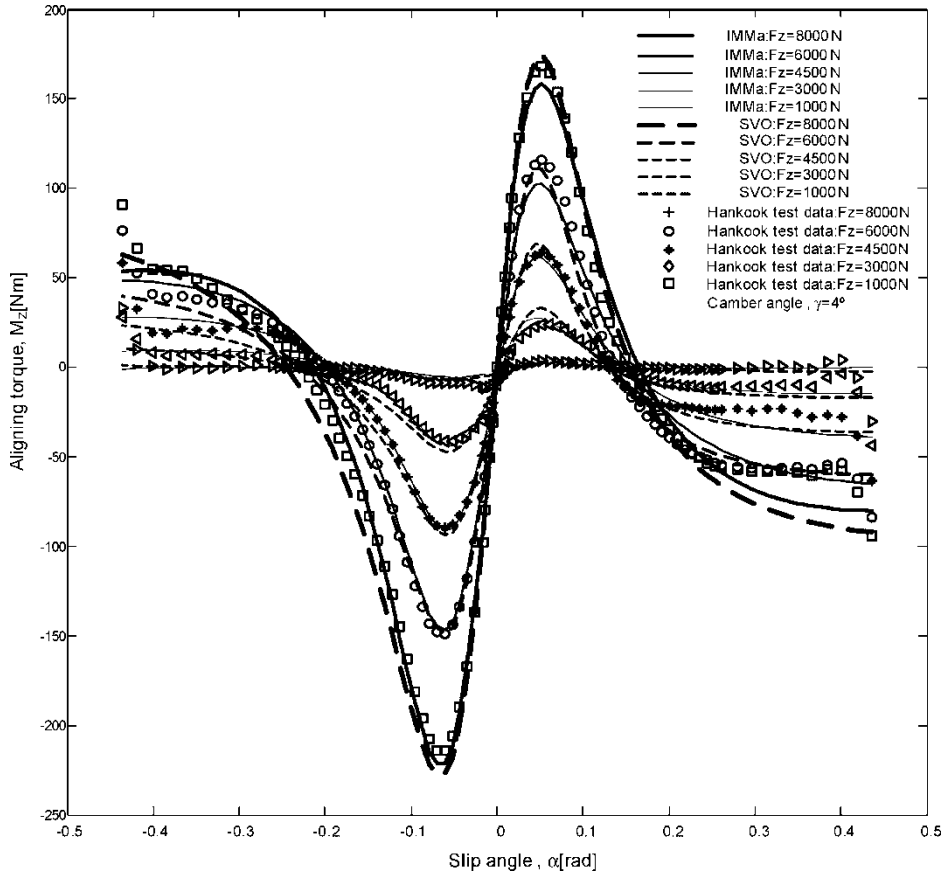


Figure 9. Aligning torque comparison obtained with parameters optimized by the IMAa algorithm and the SVO with respect to  $\gamma = 4^\circ$  test data.

case, the computational cost in time was much higher than in other cases owing to the huge number of test data and parameters to be optimized, which played a role.

### 3.4 Case IV

The results obtained in the cases where the slip angle is equal to  $2^\circ$ ,  $4^\circ$  and  $8^\circ$  are presented in figures 11–13, respectively. Here, it is possible to observe the different adjustment that the Magic Formula for combined slip has to the tyre test data if the IOA and the SVO are used to optimize the Magic Formula parameters.

Note that in the graphic result representation in figures 11–13, there are not 139 test points represented for every vertical load, with the objective to clarify the figure.

For the Magic Formula Delft Tyre 96 version, the longitudinal force parameters optimized by our algorithm and the ones obtained by the SVO are presented in table 16.

The algorithm took a computational time of 5 min 16 s when  $n$  was 139 points,  $m$  was three load cases and  $p$  was seven slip angles cases. The computational time is highly dependent on the number of points where the goal function is minimized, and the number of parameters to be optimized is an influential element in the computational cost.

With the aim to evaluate the quality of adjustment to the tyre test data, we have evaluated the sum-squared differences between the longitudinal forces with the parameters optimized



Table 10. Parameters for aligning torque (pure side slip) of the Magic Formula Delft Tyre 96 version.

Aligning torque coefficients	SVO	IMMa algorithm
QBZ1: $B_{pt}$ trail slope factor for trail at $F_{znom}$	11.266	10.47871
QBZ2: $B_{pt}$ slope variation with load	2.806	-2.04739
QBZ3: $B_{pt}$ slope variation with square load	-0.586	6.09958
QBZ4: $B_{pt}$ slope variation with camber	0.405	0.39191
QBZ5: $B_{pt}$ slope variation with absolute camber	-0.020833	-0.01279
QCZ1: $C_{pt}$ shape factor for pneumatic trail	1.1908	1.18899
QDZ1: Peak trail $D''_{pt} = D_{pt}^*(F_z/F_{znom} \times R_0)$	0.11738	0.11411
QDZ2: $D''_{pt}$ peak variation with load	0.009433	0.00479
QDZ3: $D''_{pt}$ peak variation with camber	0.13701	0.12582
QDZ4: $D''_{pt}$ peak variation with square camber	-2.8255	-1.10927
QEZ1: $E_{pt}$ trail curvature at $F_{znom}$	-2.3346	-2.88862
QEZ2: $E_{pt}$ curvature variation with load	1.7478	-0.83490
QEZ3: $E_{pt}$ curvature variation with square load	0	3.71462
QEZ4: $E_{pt}$ curvature variation with $\alpha$ -t sign	0.25	0.15337
QEZ5: $E_{pt}$ curvature variation with camber and $\alpha$ -t sign	2.1345	1.33032
QHZ1: $S_{ht}$ horizontal shift for trail at $F_{znom}$	2.5437E-4	0.00024
QHZ2: $S_{ht}$ shift variation with load	3.316E-4	0.00102
QHZ3: $S_{ht}$ shift variation with camber	0.08772	0.12610
QHZ4: $S_{ht}$ shift variation with camber and load	0.04964	0.01917
QBZ9: $B_r$ slope factor of $M_{zr}$ residual torque	29.996	17.87469
QBZ10: $B_r$ slope factor of $M_{zr}$ residual torque	0	5.66140
QDZ6: $D''_{mr} = D_{mr}/(F_z \times R_0)$ peak residual torque	-7.047E-4	-0.00049
QDZ7: $D''_{mr}$ peak factor variation with load	1.8184E-4	0.00025
QDZ8: $D''_{mr}$ peak factor variation with camber	-0.15867	-0.18840
QDZ9: $D''_{mr}$ peak factor variation with camber and load	-0.02444	0.00415

Table 11. Sum-squared error from aligning torque curve to aligning torque test data.

Sum-squared error ( $N^2m^2$ )		
	$\sum_{i=1}^n \sum_{j=1}^m \sum_{g=1}^l [M_{Z0}^{IMMa \text{ algorithm}} - M_{Z0}^{measured}]^2$	$\sum_{i=1}^n \sum_{j=1}^m \sum_{g=1}^l [M_{Z0}^{SVO} - M_{Z0}^{measured}]^2$
$F_z = [8000, 6000, 4500, 3000, 1000]N$ $-25^\circ \leq \alpha \leq 25^\circ$ $\gamma = [-4, -2, -1, 0, 1, 2, 4]^\circ$	108615	167025
$F_z = [8000, 6000, 4500]N$ $-25^\circ \leq \alpha \leq 25^\circ$ $\gamma = [-4, 0, 4]^\circ$	2978	10080

Table 12. MSE from aligning torque curve to aligning torque test data expressed in rate percentage for all vertical loads and all camber angles.

% MSE		
	$\sqrt{\left[ \frac{\sum_{i=1}^n (M_{Z0}^{IMMa \text{ algorithm}} - M_{Z0}^{measured})^2}{\sum_{i=1}^n (M_{Z0}^{measured})^2} \right]}$	$\sqrt{\left[ \frac{\sum_{i=1}^n (M_{Z0}^{SVO} - M_{Z0}^{measured})^2}{\sum_{i=1}^n (M_{Z0}^{measured})^2} \right]}$
$F_z = [8000, 6000, 4500, 3000, 1000]N$ $-25^\circ \leq \alpha \leq 25^\circ$ $\gamma = [-4, -2, -1, 0, 4, 2, 1]^\circ$	30.01	31.99

Table 13. MSE from aligning torque curve to aligning torque test data expressed in rate percentage.

	% MSE	
	$\sqrt{\left[ \frac{\sum_{i=1}^n (M_{Z0}^{IMMa \text{ algorithm}} - M_{Z0}^{\text{measured}})^2}{\sum_{i=1}^n (M_{Z0}^{\text{measured}})^2} \right]}$	$\sqrt{\left[ \frac{\sum_{i=1}^n (M_{Z0}^{SVO} - M_{Z0}^{\text{measured}})^2}{\sum_{i=1}^n (M_{Z0}^{\text{measured}})^2} \right]}$
$\gamma = 0^\circ$		
$F_z = 8000 \text{ N}$	6.28	10.98
$F_z = 6000 \text{ N}$	8.08	10.27
$F_z = 4500 \text{ N}$	12.33	13.50
$F_z = 3000 \text{ N}$	28.09	29.76
$F_z = 1000 \text{ N}$	83.04	83.14
Total	29.57	29.53

Table 14. MSE from aligning torque curve to aligning torque test data expressed in rate percentage.

	% MSE	
	$\sqrt{\left[ \frac{\sum_{i=1}^n (M_{Z0}^{IMMa \text{ algorithm}} - M_{Z0}^{\text{measured}})^2}{\sum_{i=1}^n (M_{Z0}^{\text{measured}})^2} \right]}$	$\sqrt{\left[ \frac{\sum_{i=1}^n (M_{Z0}^{SVO} - M_{Z0}^{\text{measured}})^2}{\sum_{i=1}^n (M_{Z0}^{\text{measured}})^2} \right]}$
$\gamma = 2^\circ$		
$F_z = 8000 \text{ N}$	5.63	10.03
$F_z = 6000 \text{ N}$	9.53	11.47
$F_z = 4500 \text{ N}$	15.66	17.55
$F_z = 3000 \text{ N}$	26.03	31.20
$F_z = 1000 \text{ N}$	84.64	85.75
Total	28.30	31.20

by the SVO and the IMMa algorithm. The results can be observed in table 17. The sum of all the differences from the test data to the longitudinal force curve obtained with the IMMa algorithm is smaller compared with the result obtained with SVO.

The MSE, between the test data and the longitudinal force curve, which correspond to the parameters obtained with every searching procedure, has been evaluated and expressed in rate percentage for the total in table 18.

The MSE for every load case and slip angles  $2^\circ$ ,  $4^\circ$  and  $8^\circ$  are shown in tables 19–21, respectively. We observe a better adjustment to the tyre test data, using the searching algorithm proposed in this article from evidence in tables 18–21.

Table 15. MSE from aligning torque curve to aligning torque test data expressed in rate percentage.

	% MSE	
	$\sqrt{\left[ \frac{\sum_{i=1}^n (M_{Z0}^{IMMa \text{ algorithm}} - M_{Z0}^{\text{measured}})^2}{\sum_{i=1}^n (M_{Z0}^{\text{measured}})^2} \right]}$	$\sqrt{\left[ \frac{\sum_{i=1}^n (M_{Z0}^{SVO} - M_{Z0}^{\text{measured}})^2}{\sum_{i=1}^n (M_{Z0}^{\text{measured}})^2} \right]}$
$\gamma = 4^\circ$		
$F_z = 8000 \text{ N}$	7.49	13.59
$F_z = 6000 \text{ N}$	9.54	12.44
$F_z = 4500 \text{ N}$	16.19	19.87
$F_z = 3000 \text{ N}$	27.03	32.96
$F_z = 1000 \text{ N}$	81.42	80.51
Total	28.33	31.87

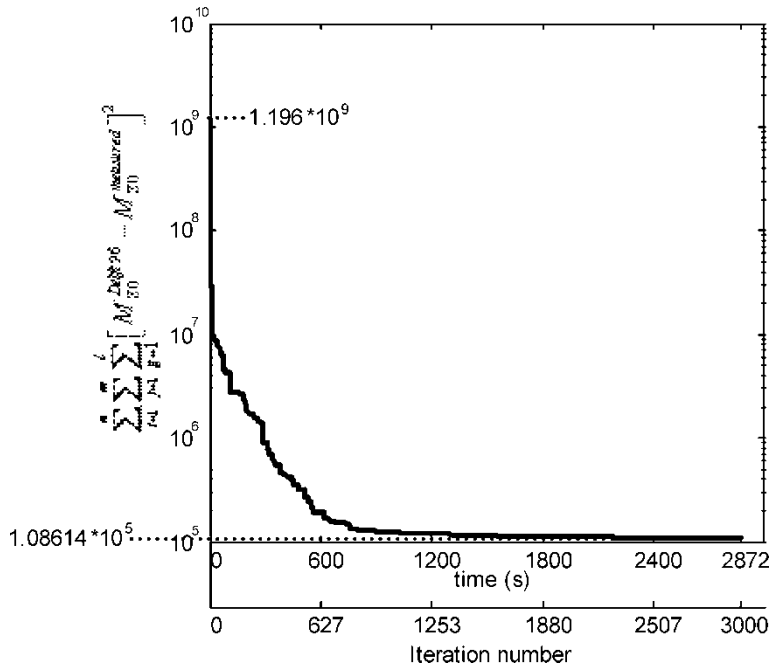


Figure 10. The sum-squared error development for the aligning torque along 3000 iterations accumulated for 82 test points for every vertical load and five vertical load cases and seven different camber angles.

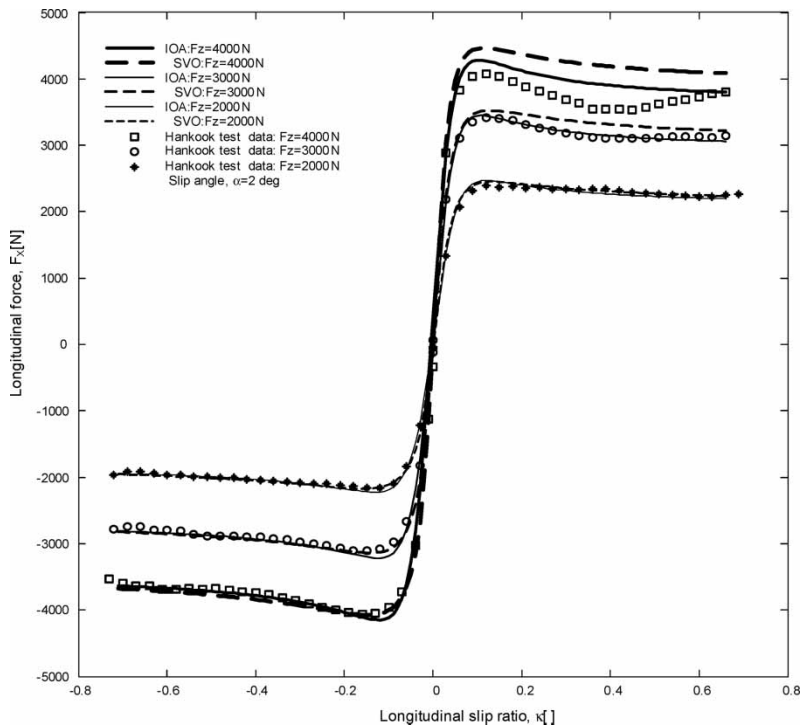


Figure 11. Longitudinal force comparison obtained with parameters optimized by the IMMa algorithm and the SVO for  $\alpha = 2^\circ$ .

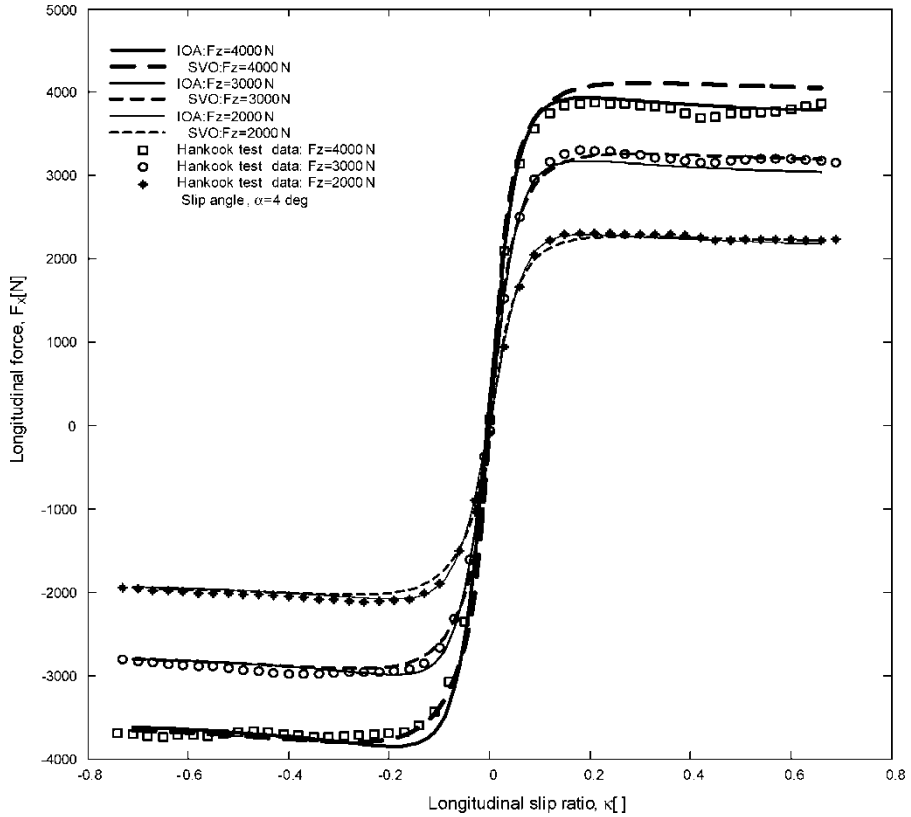


Figure 12. Longitudinal force comparison obtained with parameters optimized by the IMM algorithm and the SVO for  $\alpha = 4^\circ$ .

During the time the algorithm worked, the sum-squared error evolved as shown in figure 14. The time the IOA spent searching the optimum parameters is overestimated. The final sum-squared error does not go down once 160 iterations have been exceeded. The algorithm took <60 s only to realize approximately 170 iterations.

### 3.5 Case V

The results obtained for slip angles  $-2^\circ$ ,  $2^\circ$ ,  $4^\circ$  and  $8^\circ$  are presented in figures 15–18, respectively. Note that, here, the test data had an irregular distribution over the slip angle.

For every slip angle, it is possible to observe the different adjustment that the lateral force of the Magic Formula for combined side slip has to the tyre test data if the IOA and the SVO are used to optimize the Magic Formula parameters.

For the Magic Formula Delft Tyre 96 version, the lateral force parameters optimized by our algorithm and the ones obtained by SVO are presented in table 22.

The algorithm took a computational time of 4 min 44 s when  $n$  was 139 points,  $m$  was three load cases and  $p$  was six slip angles.

With the objective to quantify the adjustment to the tyre test data, we have evaluated the sum-squared differences between the lateral forces with the parameters optimized by the SVO and the IMM algorithm. The results can be observed in table 23. The sum of all the differences from the test data to the lateral force curve obtained with the IMM algorithm is 40% smaller than the error obtained with SVO.

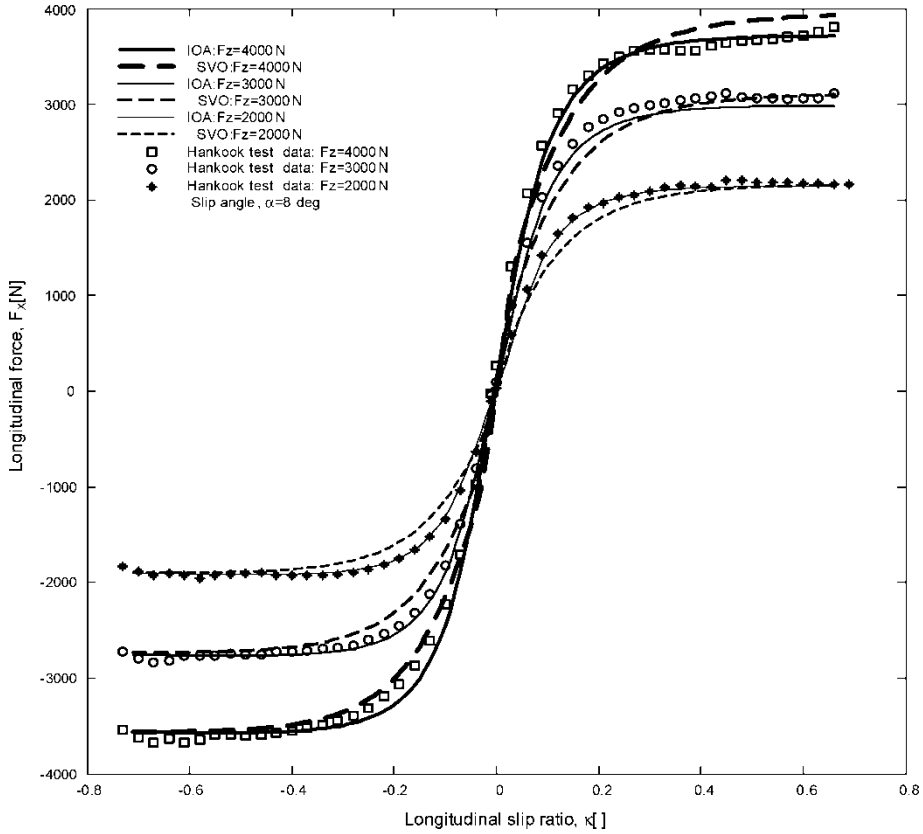


Figure 13. Longitudinal force comparison obtained with parameters optimized by the IMM algorithm and the SVO for  $\alpha = 8^\circ$ .

Table 16. Longitudinal force parameters (combined slip) of the Magic Formula Delft Tyre 96 version.

Longitudinal coefficients	SVO	IMM algorithm
RBX1: slope factor of $F_x$ reduction for combined slip	13.458	24.8565
RBX2: slope variation of $F_x$ reduction with $\kappa$	-11.604	22.43545
RCX1: slope factor of $F_x$ reduction for combined slip	1.1666	1.00542
RHX1: shift factor of $F_x$ reduction for combined slip	0.0040974	0.00344

Table 17. Sum-squared error from the longitudinal force curve to the longitudinal force test data.

	Sum-squared error ( $N^2$ )	
	$\sum_{i=1}^n \sum_{j=1}^m \sum_{f=1}^p [F_x^{\text{IMM algorithm}} - F_x^{\text{measured}}]^2$	$\sum_{i=1}^n \sum_{j=1}^m \sum_{f=1}^p [F_x^{\text{SVO}} - F_x^{\text{measured}}]^2$
$F_z = [4000, 3000, 2000] \text{ N}$ $-0.71 \leq \kappa \leq 0.66$ $\alpha = [-2, -4, -8, 0, 2, 4, 8]$	$3.600788 \times 10^9$	$3.625239 \times 10^9$

Table 18. MSE from the longitudinal force curve to the longitudinal force tyre test data expressed in rate percentage for all vertical loads and all slip angles.

	% MSE total	
	$\sqrt{\left[ \frac{\sum_{i=1}^n (F_x^{\text{IMMa algorithm}} - F_x^{\text{measured}})^2}{\sum_{i=1}^n (F_x^{\text{measured}})^2} \right]}$	$\sqrt{\left[ \frac{\sum_{i=1}^n (F_x^{\text{SVO}} - F_x^{\text{measured}})^2}{\sum_{i=1}^n (F_x^{\text{measured}})^2} \right]}$
$F_z = [4000, 3000, 2000] \text{ N}$ $-71 \leq \kappa \leq 0.66$ $\alpha = [-2, -4, -8, 0, 2, 4, 8]^\circ$	3.72	4.87

Table 19. MSE from the longitudinal force curve to the longitudinal force tyre test data expressed in rate percentage when  $\alpha = 2^\circ$ .

	% MSE	
$\alpha = 4^\circ$	$\sqrt{\left[ \frac{\sum_{i=1}^n (F_x^{\text{IMMa algorithm}} - F_x^{\text{measured}})^2}{\sum_{i=1}^n (F_x^{\text{measured}})^2} \right]}$	$\sqrt{\left[ \frac{\sum_{i=1}^n (F_x^{\text{SVO}} - F_x^{\text{measured}})^2}{\sum_{i=1}^n (F_x^{\text{measured}})^2} \right]}$
$F_z = 4000 \text{ N}$	7.41	9.26
$F_z = 3000 \text{ N}$	2.75	3.98
$F_z = 2000 \text{ N}$	2.12	2.09
Total	4.09	5.11

Table 20. MSE from the longitudinal force curve to the longitudinal force tyre test data expressed in rate percentage when  $\alpha = 4^\circ$ .

	% MSE	
$\alpha = 4^\circ$	$\sqrt{\left[ \frac{\sum_{i=1}^n (F_x^{\text{IMMa algorithm}} - F_x^{\text{measured}})^2}{\sum_{i=1}^n (F_x^{\text{measured}})^2} \right]}$	$\sqrt{\left[ \frac{\sum_{i=1}^n (F_x^{\text{SVO}} - F_x^{\text{measured}})^2}{\sum_{i=1}^n (F_x^{\text{measured}})^2} \right]}$
$F_z = 4000 \text{ N}$	4.47	5.67
$F_z = 3000 \text{ N}$	2.21	2.61
$F_z = 2000 \text{ N}$	3.23	3.21
Total	3.3	3.83

Table 21. MSE from the longitudinal force curve to the longitudinal force tyre test data expressed in rate percentage when  $\alpha = 8^\circ$ .

	% MSE	
$\alpha = 8^\circ$	$\sqrt{\left[ \frac{\sum_{i=1}^n (F_x^{\text{IMMa algorithm}} - F_x^{\text{measured}})^2}{\sum_{i=1}^n (F_x^{\text{measured}})^2} \right]}$	$\sqrt{\left[ \frac{\sum_{i=1}^n (F_x^{\text{SVO}} - F_x^{\text{measured}})^2}{\sum_{i=1}^n (F_x^{\text{measured}})^2} \right]}$
$F_z = 4000 \text{ N}$	4.64	4.92
$F_z = 3000 \text{ N}$	2.16	5.03
$F_z = 2000 \text{ N}$	2.4	5.83
Total	3.07	5.26

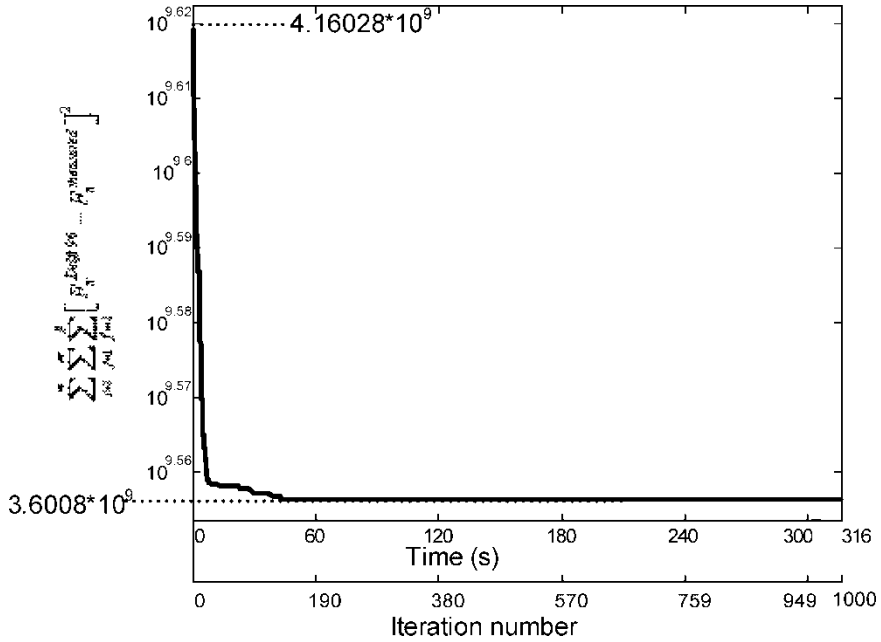


Figure 14. Development of the sum-squared error for longitudinal force along 1000 iterations and accumulated for 139 points and three vertical load cases and seven slip angles.

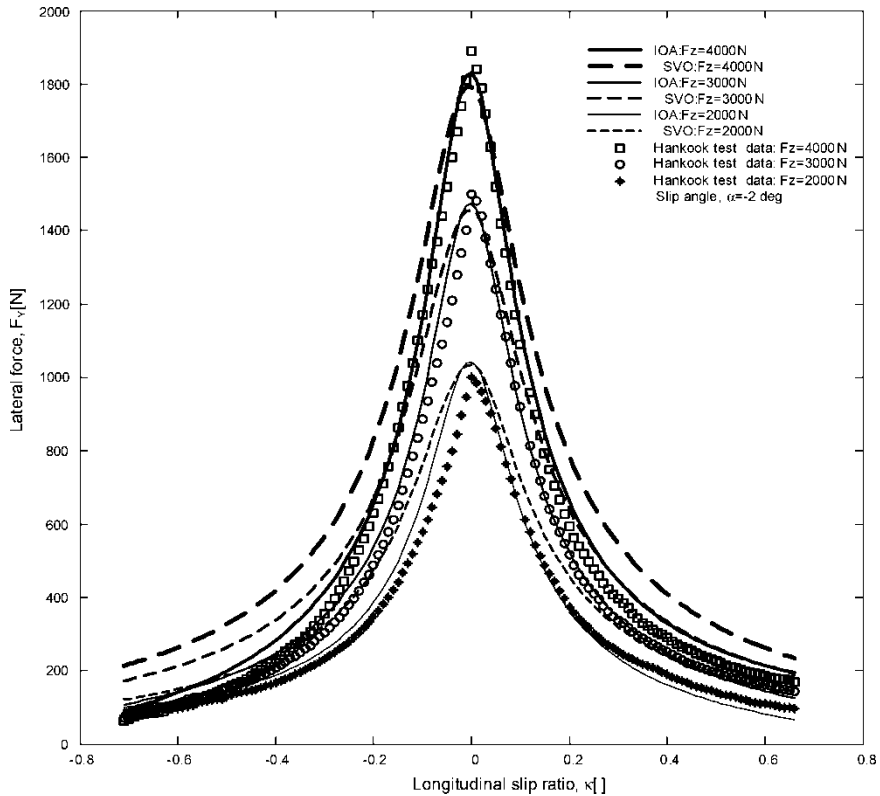


Figure 15. Lateral force comparison obtained with the parameters optimized by the IMM algorithm and the SVO with respect to  $\alpha = -2^\circ$  test data.

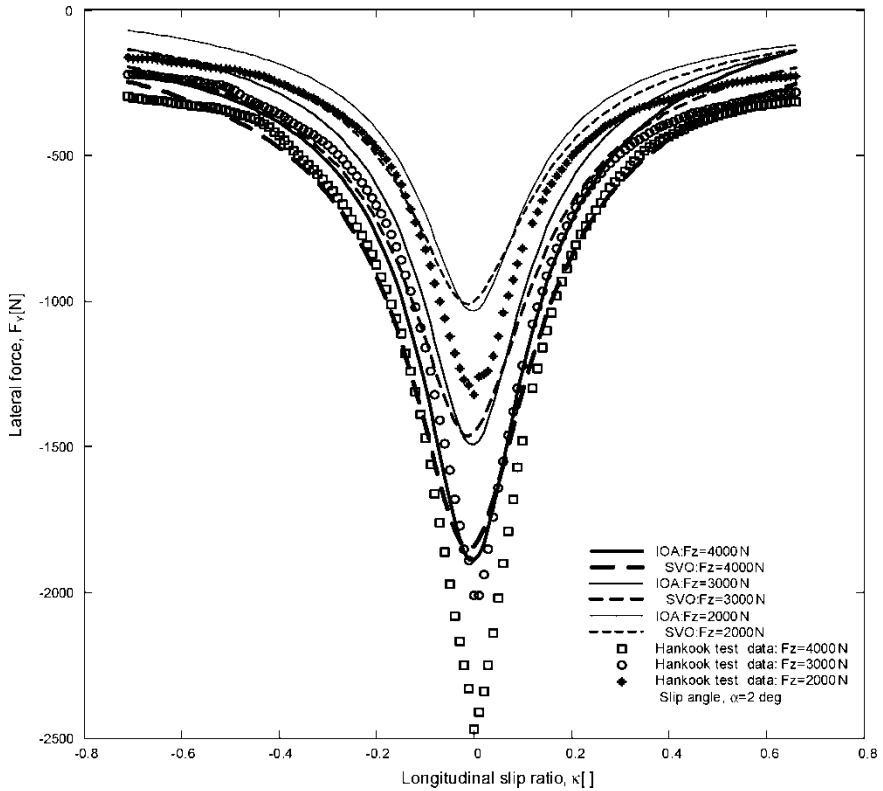


Figure 16. Lateral force comparison obtained with the parameters optimized by the IMMa algorithm and the SVO with respect to  $\alpha = 2^\circ$  test data.

The MSE between the lateral force test data and the lateral force curve obtained with the parameters that correspond to every searching procedure has been evaluated and expressed in rate percentage for the total in table 24, and every vertical load case and every slip angle is shown in tables 25–28.

For the  $\alpha$  slip angles  $-2^\circ$ ,  $-4^\circ$ ,  $-8^\circ$ ,  $2^\circ$ ,  $4^\circ$ , and  $8^\circ$ , we observe a better adjustment to the lateral force test data, using the searching algorithm proposed in this article, based on genetics than the adjustment obtained using the parameters optimized by the SVO.

On this occasion, the MSE is very high owing to a bad behaviour in the test data. When  $\alpha = 2^\circ$ , the test data are not symmetric with respect to  $y = 0$  axis compared with those when  $\alpha = -2^\circ$ .

During the time the algorithm worked, the sum-squared error for lateral force evolved as shown in figure 19. The time the IOA spent searching the optimum  $Y$  parameters is overestimated. The final sum-squared error does not decrease once 135 iterations have been exceeded. The algorithm took only 40 s to realize 135 iterations, to obtain the final solution.

#### 4. Method attributes

In each case, the best solution was found for NP, CP, MP,  $F$ , range and itermax shown in table 29. The initial values used by the algorithm for the parameters to be optimized were



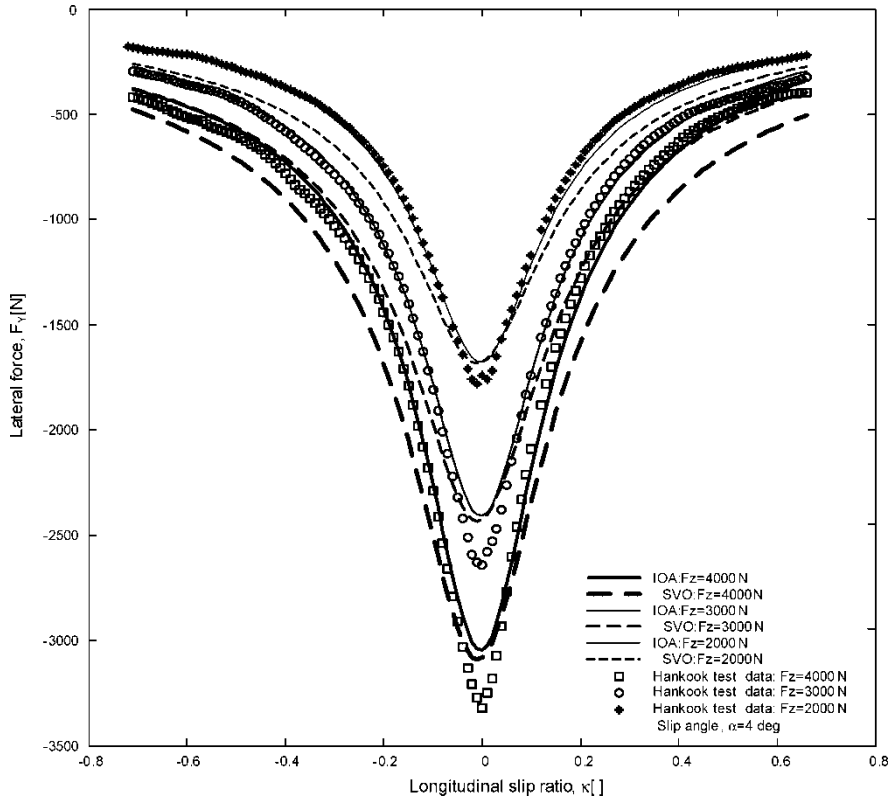


Figure 17. Lateral force comparison obtained with the parameters optimized by the IMMa and the SVO with respect to  $\alpha = 4^\circ$  test data.

randomly chosen by the computer code in the range [0, 1]. However, it was verified that the reached solution was always very similar for those cases and any other tested cases. This fact points out that the method escapes local minimums when the number of evaluations is large enough.

It is observed that the iteration numbers required by genetic algorithms is generally much larger than the iterations used by gradient-based methods. However, the function evaluation is much more complex for analytical methods (gradient-based methods), which need the computation of first-order derivatives of the objective functions. Thus, the computation time of the genetic algorithms is lower, in general.

It is necessary to remark that the values used for NP,  $F$ , CP, MP and mutation range correspond with the best found for these cases. The influences of the values of those parameters will be treated in future papers.

In table 30, the time, the number of test data points used for the optimization, parameter numbers optimized and test data employed for every case are shown.

## 5. Conclusions

The Magic Formula Tyre model for the description of steady tyre behaviour in vehicle dynamics simulations is very accurate and widely used, but the determination of the Magic Formula

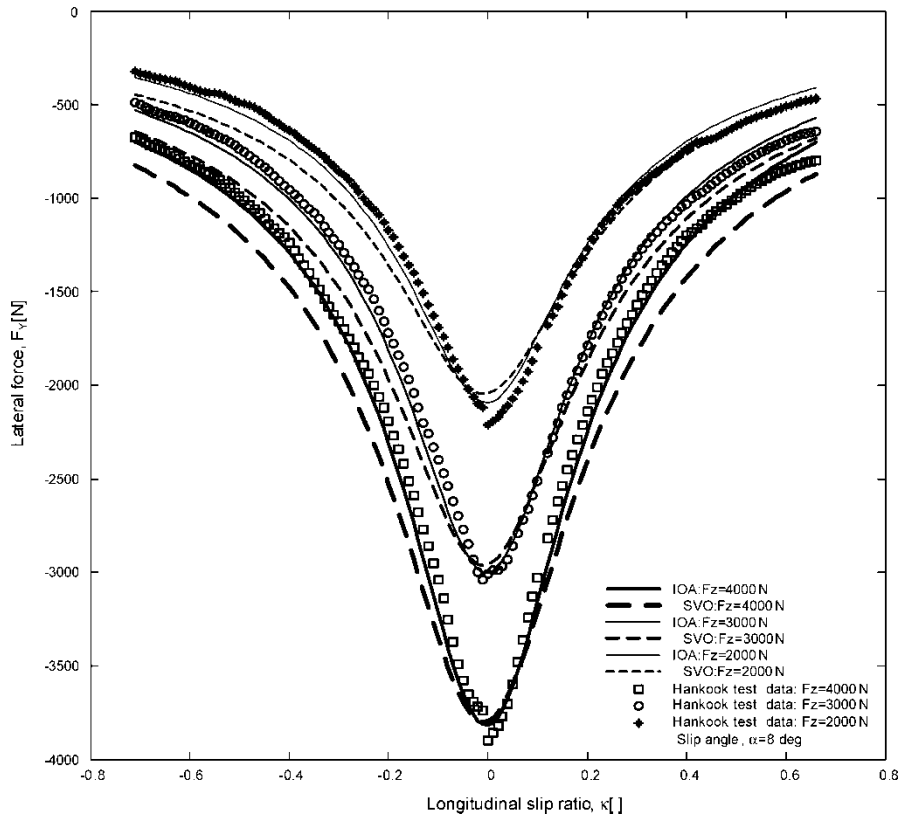


Figure 18. Lateral force comparison obtained with the parameters optimized by the IMM algorithm and the SVO with respect to  $\alpha = 8^\circ$  test data.

parameters may be difficult. This article deals with a new method based on evolutionary techniques to determine the Magic Formula parameters, with no need of special mathematical knowledge of optimization processes, nor physical knowledge of the meaning of the Magic Formula parameters, nor its contributions and interrelation among them. A set of problems of difficult solution for the vehicle dynamics research groups are those together with the selection of the starting values to initialize the optimization.

Table 22. Lateral force parameters (combined slip) of the Magic Formula Delft Tyre 96 version.

Lateral coefficients	SVO	IMM algorithm
RBV1: Slope factor for combined $F_y$ reduction	9.58	11.14388
RBV2: Slope variation of $F_y$ reduction with $\alpha$	8.813	10.14162
RBV3: Shift term for $\alpha$ in slope of $F_y$ reduction	-0.014943	-0.015481
RCV1: Shape factor for combined $F_y$ reduction	1.0203	1.038732
RHV1: Shift factor for combined $F_y$ reduction	0.007964	0.0031137
RVY1: $\kappa$ induced side force $S_{vyk}/M_{uy} \times F_z$ at $F_{znom}$	-0.01058	-1.485137
RVY2: Variation of $S_{vyk}/M_{uy} \times F_z$ with load	0.0333	-4.425144
RVY3: Variation of $S_{vyk}/M_{uy} \times F_z$ with camber	-0.825	0.680957
RVY4: Variation of $S_{vyk}/M_{uy} \times F_z$ with $\alpha$	116.72	10.72882
RVY5: Variation of $S_{vyk}/M_{uy} \times F_z$ with $\kappa$	1.9	-0.201998
RVY6: Variation of $S_{vyk}/M_{uy} \times F_z$ with $\tan(\kappa)$	-27.59	0.083549

Table 23. Sum squared error from lateral force curve to lateral force test data.

	Sum-squared error (N <sup>2</sup> )	
	$\sum_{i=1}^n \sum_{j=1}^m \sum_{f=1}^p \left[ F_y^{\text{IMMa algorithm}} - F_y^{\text{measured}} \right]^2$	$\sum_{i=1}^n \sum_{j=1}^m \sum_{f=1}^p \left[ F_y^{\text{SVO}} - F_y^{\text{measured}} \right]^2$
$F_z = [4000, 3000, 2000] \text{ N}$ $-0.71 \leq \kappa \leq 0.66$ $\alpha = [-2, -4, -8, 2, 4, 8]^\circ$	$2.3835 \times 10^7$	$6.045 \times 10^7$

In this article, the IOA, which is suitable for the determination of the Magic Formula parameters, has been verified. This method was implemented to obtain the parameters of the Magic Formula version called Delft Tyre 96. The braking and traction force and the lateral force and aligning torque at pure and combined manoeuvres were obtained successfully. The Magic Formula was adjusted to test data for all the cases, with a lower error level than other methods based on traditional optimization methods such as Levenberg–Marquart used in ref. [12].

The discussion about the method employed here, in relation with other analytical optimization methods such as neuro-tyre optimization process [13] and Nelder and Mead [14], has been done in Cabrera *et al.* [8]. In this article, it is verified that, using these traditional searching methods, if the initial values of the parameters to be optimized are far from the optimum, the final error is bigger than the error made by the IOA and if the initial values are near the optimum, the final error is of the same magnitude as the error made by IOA but continued being bigger.

Table 24. MSE from lateral force curve to lateral force test data expressed in rate percentage for all vertical loads and all slip angles.

	% MSE	
	$\sqrt{\left[ \frac{\sum_{i=1}^n (F_y^{\text{IMMa algorithm}} - F_y^{\text{measured}})^2}{\sum_{i=1}^n (F_y^{\text{measured}})^2} \right]}$	$\sqrt{\left[ \frac{\sum_{i=1}^n (F_y^{\text{SVO}} - F_y^{\text{measured}})^2}{\sum_{i=1}^n (F_y^{\text{measured}})^2} \right]}$
$F_z = [4000, 3000, 2000] \text{ N}$ $-0.71 \leq \kappa \leq 0.66$ $\alpha = [-2, -4, -8, 2, 4, 8]^\circ$	9.15	14.88

Table 25. MSE from the lateral force curve to the lateral force test data expressed in rate percentage when  $\alpha = -2^\circ$ .

	% MSE	
	$\sqrt{\left[ \frac{\sum_{i=1}^n (F_y^{\text{IMMa algorithm}} - F_y^{\text{measured}})^2}{\sum_{i=1}^n (F_y^{\text{measured}})^2} \right]}$	$\sqrt{\left[ \frac{\sum_{i=1}^n (F_y^{\text{SVO}} - F_y^{\text{measured}})^2}{\sum_{i=1}^n (F_y^{\text{measured}})^2} \right]}$
$\alpha = -2^\circ$		
$F_z = 4000 \text{ N}$	5.75	21.63
$F_z = 3000 \text{ N}$	6.20	21.16
$F_z = 2000 \text{ N}$	9.45	22.27
Total	7.13	21.69

Table 26. MSE from the lateral force curve to the lateral force test data expressed in rate percentage when  $\alpha = 2^\circ$ .

	% MSE	
	$\sqrt{\left[ \frac{\sum_{i=1}^n (F_y^{\text{IMMa algorithm}} - F_y^{\text{measured}})^2}{\sum_{i=1}^n (F_y^{\text{measured}})^2} \right]}$	$\sqrt{\left[ \frac{\sum_{i=1}^n (F_y^{\text{SVO}} - F_y^{\text{measured}})^2}{\sum_{i=1}^n (F_y^{\text{measured}})^2} \right]}$
$\alpha = 2^\circ$		
$F_z = 4000 \text{ N}$	20.82	15.08
$F_z = 3000 \text{ N}$	23.94	17.91
$F_z = 2000 \text{ N}$	24.72	17.27
Total	23.16	16.75

The MSE calculated for every case studied before has a relative meaning and it is a way to compare both the optimization methods. Note that MSE values are not an absolute indicator by themselves because of the fact that when the vertical load tends to zero the MSE tends to go up, whereas the differences keep the same magnitude to test data for all vertical loads.

The main advantages of the proposed method are the simplicity of the algorithm implementation and the option of starting the optimization process with any initial values for the parameters. Consequently, the required experience for users of the method diminishes significantly and substantially.

The time the IOA spent to obtain the optimal solution was highly dependent on the test data number and the number of tyre model parameters.

The number of tyre model parameters increases from 14 for longitudinal force to 18 for lateral force and to 25 for aligning torque for pure slip and from four for longitudinal force

Table 27. MSE from the lateral force curve to the lateral force test data expressed in rate percentage when  $\alpha = 4^\circ$ .

	% MSE	
	$\sqrt{\left[ \frac{\sum_{i=1}^n (F_y^{\text{IMMa algorithm}} - F_y^{\text{measured}})^2}{\sum_{i=1}^n (F_y^{\text{measured}})^2} \right]}$	$\sqrt{\left[ \frac{\sum_{i=1}^n (F_y^{\text{SVO}} - F_y^{\text{measured}})^2}{\sum_{i=1}^n (F_y^{\text{measured}})^2} \right]}$
$\alpha = 4^\circ$		
$F_z = 4000 \text{ N}$	5.70	13.59
$F_z = 3000 \text{ N}$	5.66	12.60
$F_z = 2000 \text{ N}$	6.56	17.03
Total	5.97	14.41

Table 28. MSE from the lateral force curve to the lateral force test data expressed in rate percentage when  $\alpha = 8^\circ$ .

	% MSE	
	$\sqrt{\left[ \frac{\sum_{i=1}^n (F_y^{\text{IMMa algorithm}} - F_y^{\text{measured}})^2}{\sum_{i=1}^n (F_y^{\text{measured}})^2} \right]}$	$\sqrt{\left[ \frac{\sum_{i=1}^n (F_y^{\text{SVO}} - F_y^{\text{measured}})^2}{\sum_{i=1}^n (F_y^{\text{measured}})^2} \right]}$
$\alpha = 8^\circ$		
$F_z = 4000 \text{ N}$	4.06	10.91
$F_z = 3000 \text{ N}$	3.98	9.64
$F_z = 2000 \text{ N}$	6.47	10.22
Total	4.84	10.26

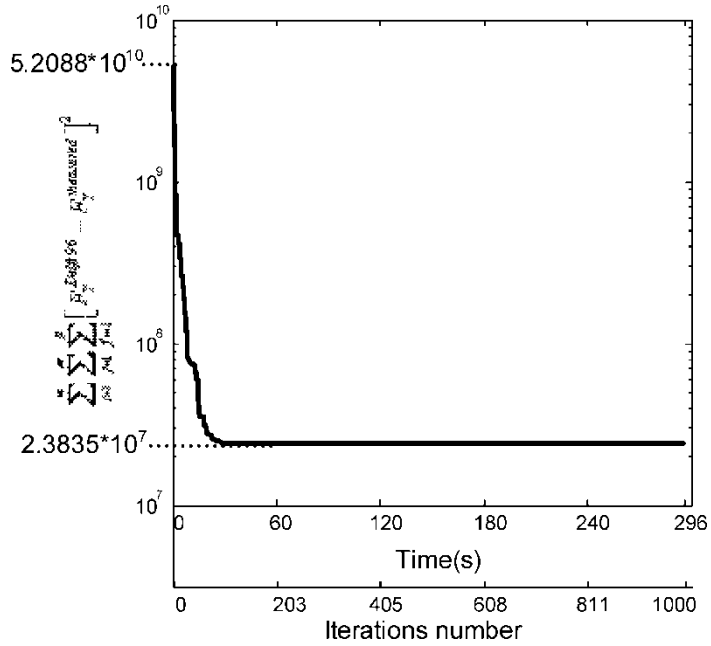


Figure 19. Sum-squared error development for lateral force along 1000 iterations accumulated for 139 test points for every vertical load and three vertical load cases and six different slip angles.

to 11 for lateral force for combined slip, but the IMM algorithm has shown its capacity to produce a better agreement to data points with a robust convergence to optimum minimum and with a low computational cost, even though the variables have an irregular distribution over the searching space.

The IOA also demonstrated a good behaviour when it was trained with an inferior number of tyre test data. The parameters obtained in this situation were also able to draw the tyre model characteristics with a good level of adjustment to the test data, even for the test data that were not used in the training process.

In spite of the fact that TNO is using constraints for the parameters, for example,  $E_X < 1$ ,  $K_{FX} > 0$ , etc., it is noted that the IOA does not need to constrain the value of the parameters to obtain optimal solutions, *i.e.* the IOA algorithm initializes the tyre model parameters randomly between  $[0, 1]$ , and the algorithm searches the suitable values of these parameters. However,

Table 29. Used parameters for IOA in this article.

	NP	D	F	CP	MP	Mutation range	Iterations number
Pure slips							
$F_x$	100	14	0.6	0.4	0.1	1	500
$F_y$	100	18	0.6	0.4	0.1	0.0003	350
$M_z$	100	25	0.6	0.4	0.1	0.0003	1250
Combined slips							
$F_X$	100	4	0.6	0.4	0.15	0.1	160
$F_Y$	100	11	0.6	0.4	0.1	0.003	135

Table 30. Time employed for the parameters optimization.

	Time (s)	Test data employed for optimization
Pure slips		
$F_x$ (14 parameters)	180	139 points for every vertical load and three vertical loads
$F_y$ (18 parameters)	60	82 points for every vertical load and five vertical loads and three camber angles
$M_z$ (25 parameters)	1200	82 points for every vertical load and five vertical loads and seven camber angles
Combined slips		
$F_x$ (4 parameters)	60	139 points for every vertical load and three vertical loads and seven slip angles
$F_y$ (11 parameters)	40	139 points for every vertical load and three vertical loads and six slip angles

if the searching space is constrained, the IOA finds the solution quicker. In the same way, the IOA does not require to establish preferred values for any parameters.

### Acknowledgements

We thank Hankook, for its selfless effort to provide the tyre test data used to realize the comparative studies in this paper.

### References

- [1] Dugoff, H., Fancher, P.S. and Segel, L., 1970, An analysis of tire traction properties and their influence on vehicle dynamic performance. *International Automobile Safety Compendium, FISITA/SAE*, Brussels, SAE No. 700377.
- [2] Gim, G. and Nikravesh, P.E., 1991, An analytical study of pneumatic tire dynamic properties, Part 1. *International Journal of Vehicle Design*, **11**(6), 589–618.
- [3] Gim, G. and Nikravesh, P.E., 1991, An analytical study of pneumatic tire dynamic properties, Part 2. *International Journal of Vehicle Design*, **12**(1), 19–39.
- [4] Gim, G. and Nikravesh, P.E., 1991, An analytical study of pneumatic tire dynamic properties, Part 3. *International Journal of Vehicle Design*, **12**(2), 217–228.
- [5] Pacejka, H.B. and Bakker, E., 1993, The magic formula tyre model. *Vehicle System Dynamics*, **21**, 1–18.
- [6] Bayle, P., Forissier, J.F. and Lafon, S., 1993, A new tyre model for vehicle dynamics simulations. *Proceedings of Automotive Technology International '93*, pp. 193–198.
- [7] Pacejka, H.B. and Besselink, I.J.M., 1997, Magic formula tyre model with transient properties. *Vehicle System Dynamics Supplement*, **27**, 234–249.
- [8] Cabrera, J.A., Ortiz, A., Carabias, E. and Simón, A., 2004, An alternative method to determine the magic formula tyre model parameters using genetic algorithms. *Vehicle System Dynamics*, **41**(2), 109–127.
- [9] Holland, J.H., 1973, Genetic algorithms and the optimal allocations of trials. *SIAM Journal of Computing*, **2**(2), 88–105.
- [10] Holland, J.H., 1975, *Adaptation in Natural and Artificial Systems* (The University of Michigan Press: Michigan).
- [11] Goldberg, D.E., 1989, *Genetic Algorithms in Search, Optimization and Machine Learning* (Addison Wesley: Massachusetts).
- [12] van Oosten, J.J.M., Savi, C., Augustin, M., Bouhet, O., Sommer, J. and Colinot, J.P., 1999, Time, tire measurements forces and moments, a new standard for steady state cornering tyre testing. *EAEC Conference*, Barcelona, 30 June–2 July.
- [13] Palkovics, L. and El-Gindy, M., 1993, Neural network representation of tyre characteristics: the neuro-tyre. *International Journal of Vehicle Design*, **14**, 563–591.
- [14] Nelder, J.A. and Mead, R., 1965, A simplex method for function minimization. *Computer Journal*, **7**, 308–313.